



*Image: 3D geography*

# Diabatic heating of mesoscale convective cloud systems from synergistic satellite data

**CHEN Xiaoting**

**Claudia Stubenrauch, Giulio Mandorli**

**Laboratoire de Météorologie Dynamique / IPSL, Paris, France**



Contact: [xiaoting.chen@lmd.ipsl.fr](mailto:xiaoting.chen@lmd.ipsl.fr)

Paris, France | 19–21 May 2025



- ◆ **Latent heat release and its fluctuations are central to the interactions within Earth's water and energy cycles, with radiative heating (RH) of upper-tropospheric (UT) clouds further enhancing this energy reservoir by at least 20%** [*Li et al. JGR, 2013, Stubenrauch et al. ACP, 2021*].
- ◆ **What is the relationship between latent heating (LH) and radiative heating in mesoscale convective systems (MCS) ?**

**TRMM** radar (2004 - 2018)

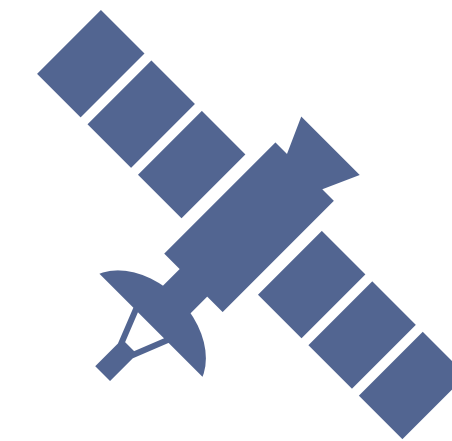
**AIRS** (2004-2018)

**IASI** (2008-2018)

IR souder

**CALIPSO** lidar (2006-2010)

**CloudSat** radar (2006-2010)

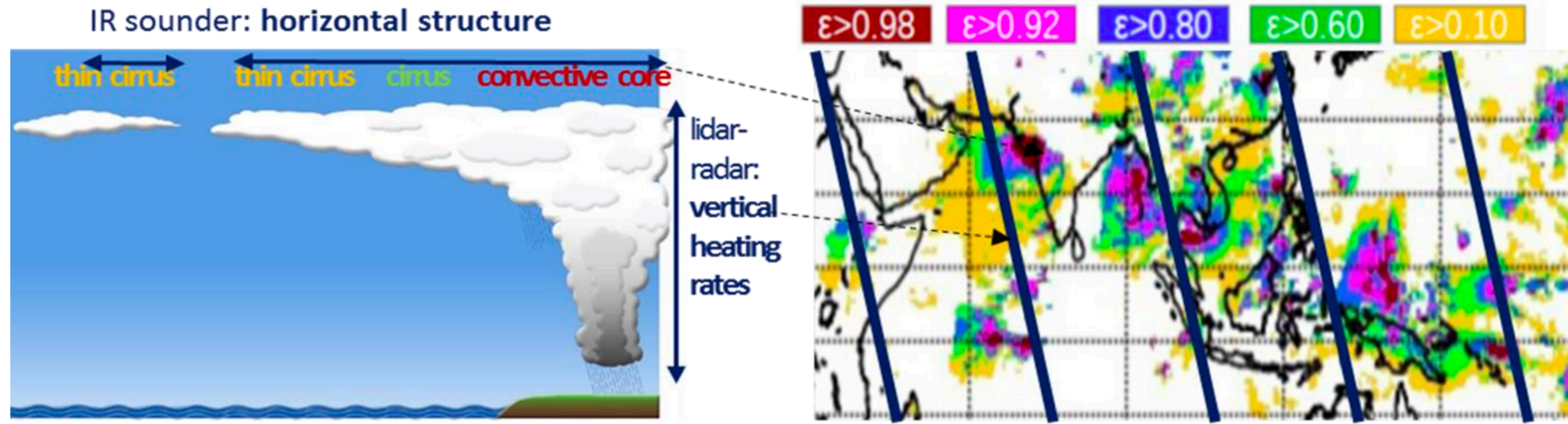


## Strategy

Complete picture -> multiple datasets

However, sophisticated measurements constrained by limited sampling density.

- Constructing a more complete dataset by Artificial Neural Network (ANN) techniques.
  - 3D Snapshots at 4 specific observation times
  - Process-oriented analyses



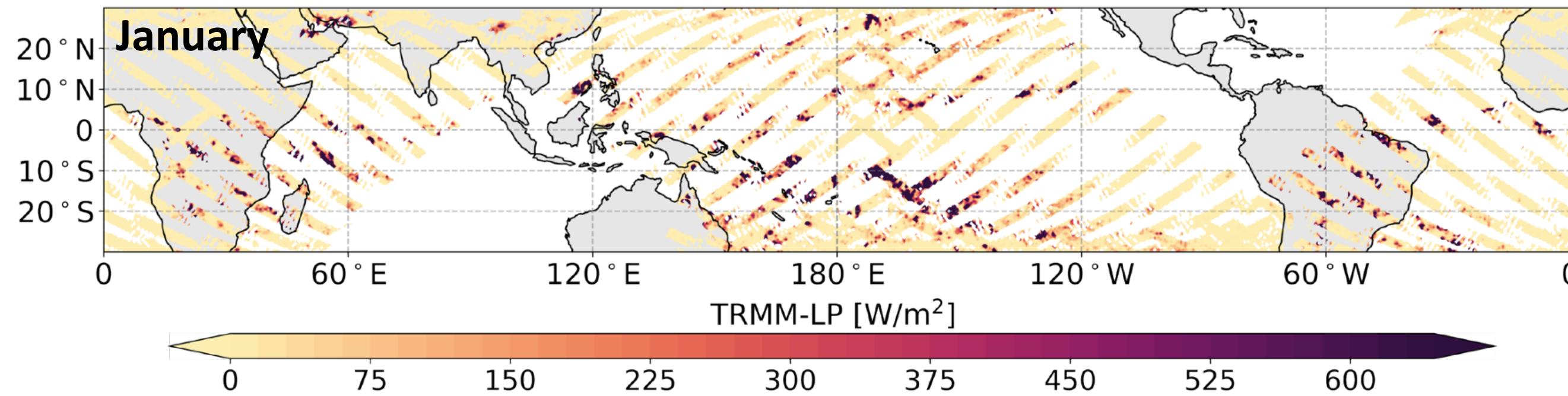
(Stubenrauch et al. 2021)

**CIRS (Clouds from IR Sounders) :**  
only cloud height & emissivity

**Vertical structure, radiative heating rate & precipitation:**  
CloudSat-CALIPSO only on narrow nadir tracks

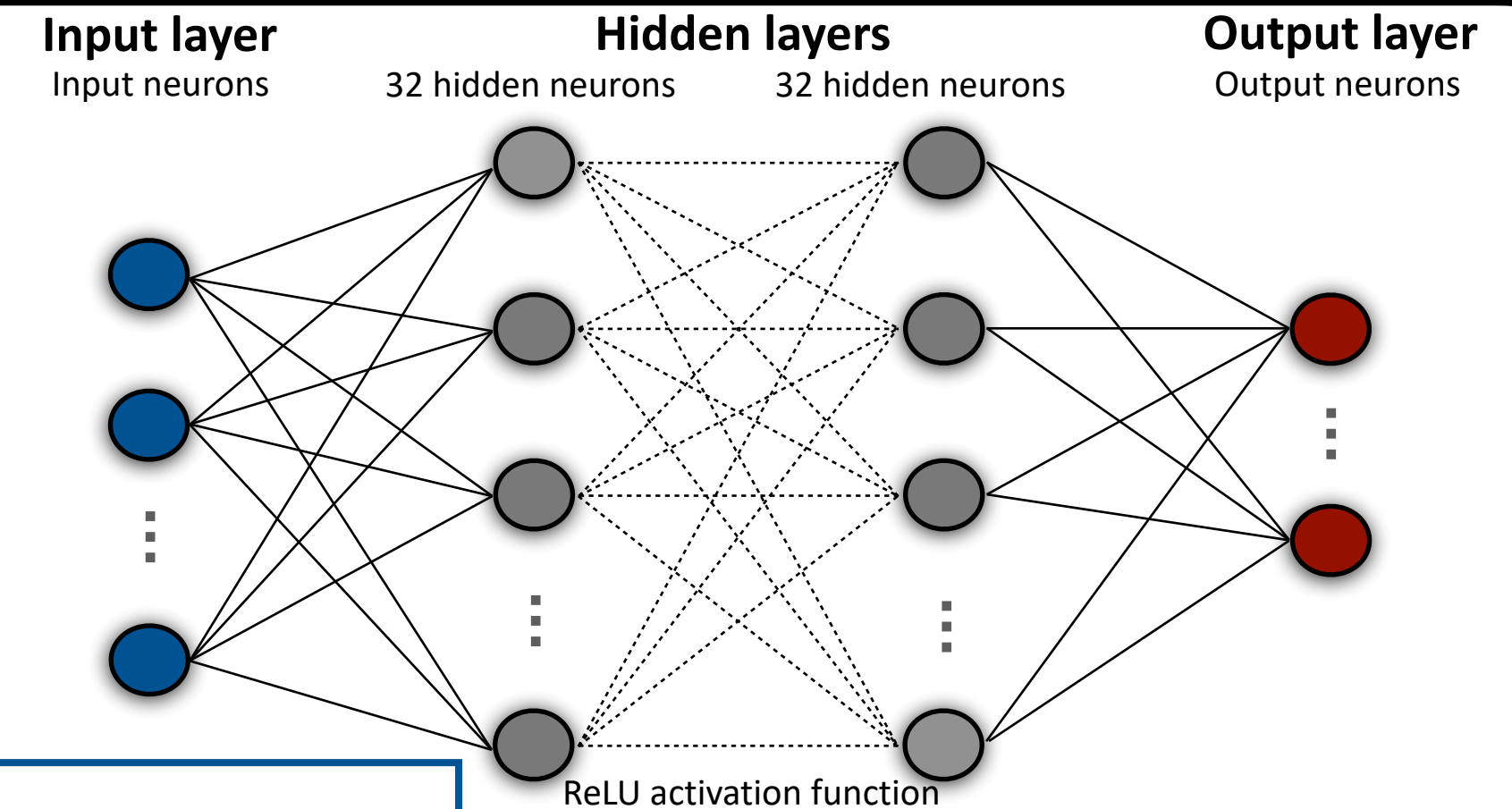
Expanded radiative heating rates are now available: <https://gewex-utcc-proes.aeris-data/fr>

## Expand *latent heating rate* across AIRS/IASI swath by ANNs



**TRMM radar statistically samples diurnal cycle, but...**  
**at specific local time (1h30 AM), only covers 3%**

AIRS swath 70%      IASI swath 77%



**Input (27 variables)**

- AIRS/IASI: CIRS cloud properties
- Grid cell structure (0.5° x 0.5°): Fractions of cloud type, clear sky, rainy area and heavy rain area.
- Re-analysis: ERA-interim atmospheric & surface properties

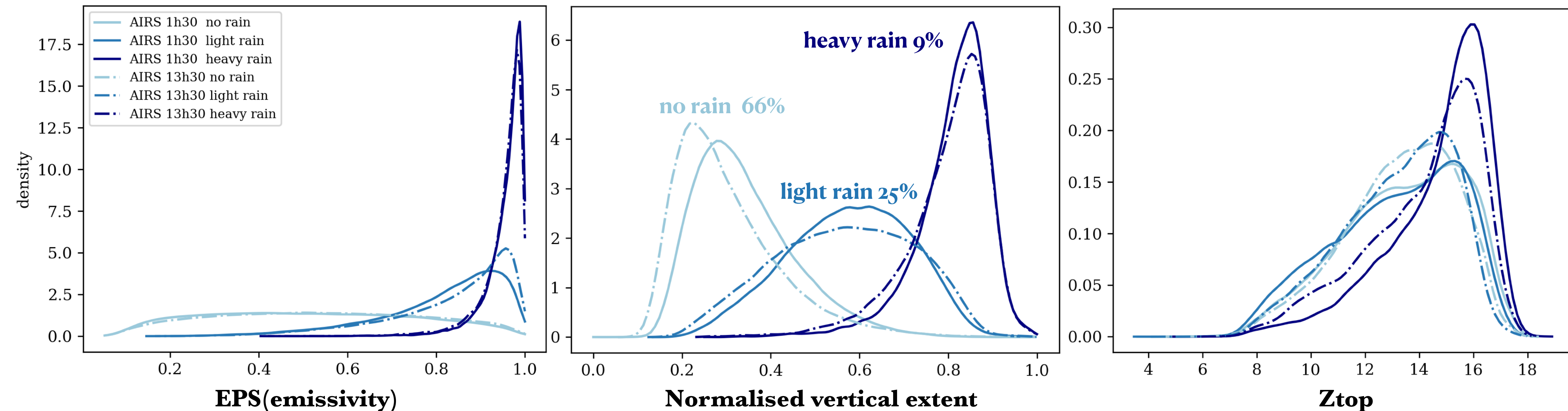
Training: 60%  
Validation: 20%  
Test: 20%

**Output**

- Latent heating rates on 20 pressure layers

**Machine learning - Artificial Neural Networks (ANNs)**

**Rain rate intensity is largest for opaque, thickest and highest clouds!**

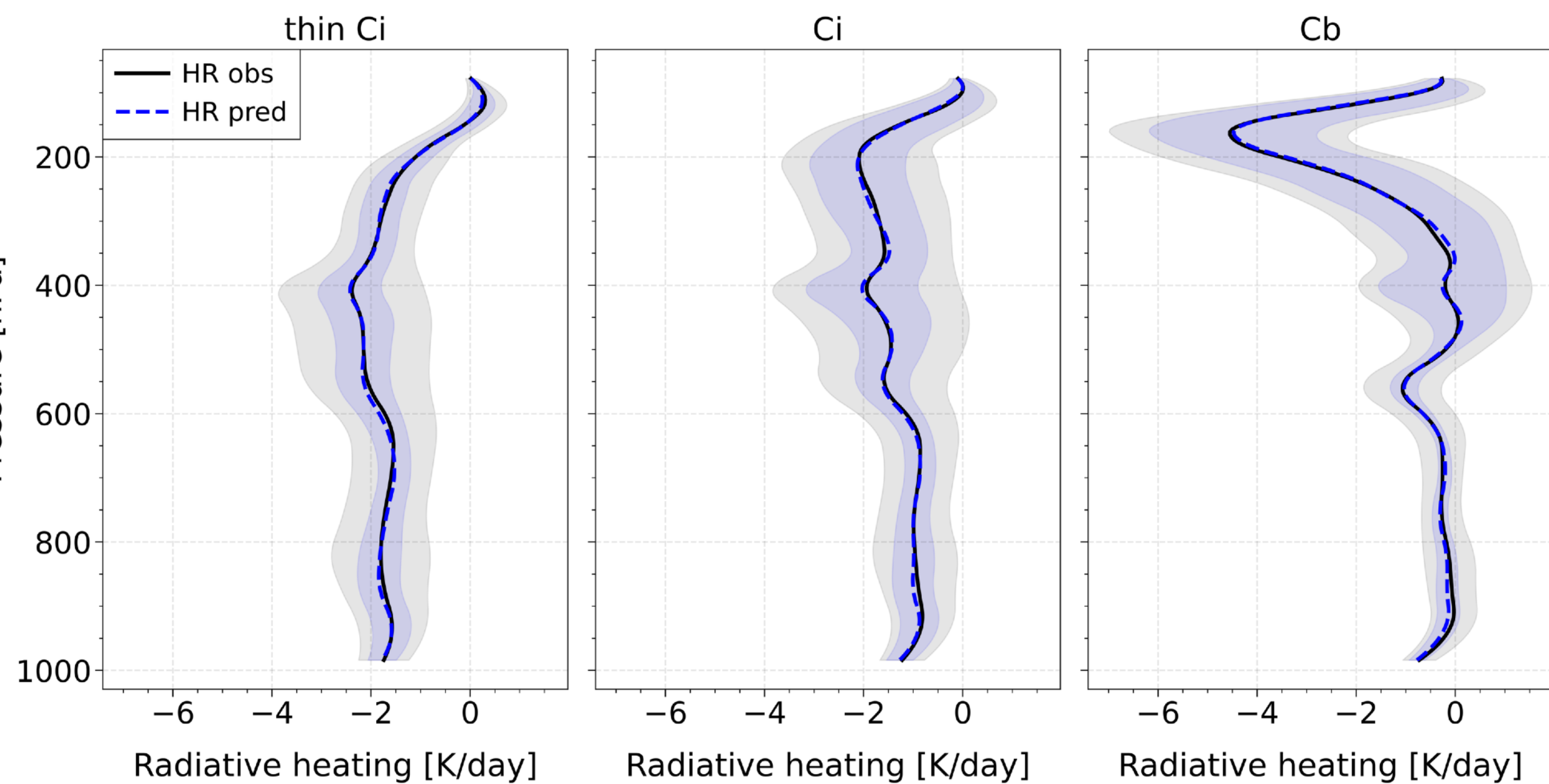


**Rain rate classification from AIRS ML-CloudSat for scene identification:** no rain, light rain, heavy rain

Good predicted mean,  
Good predicted variability



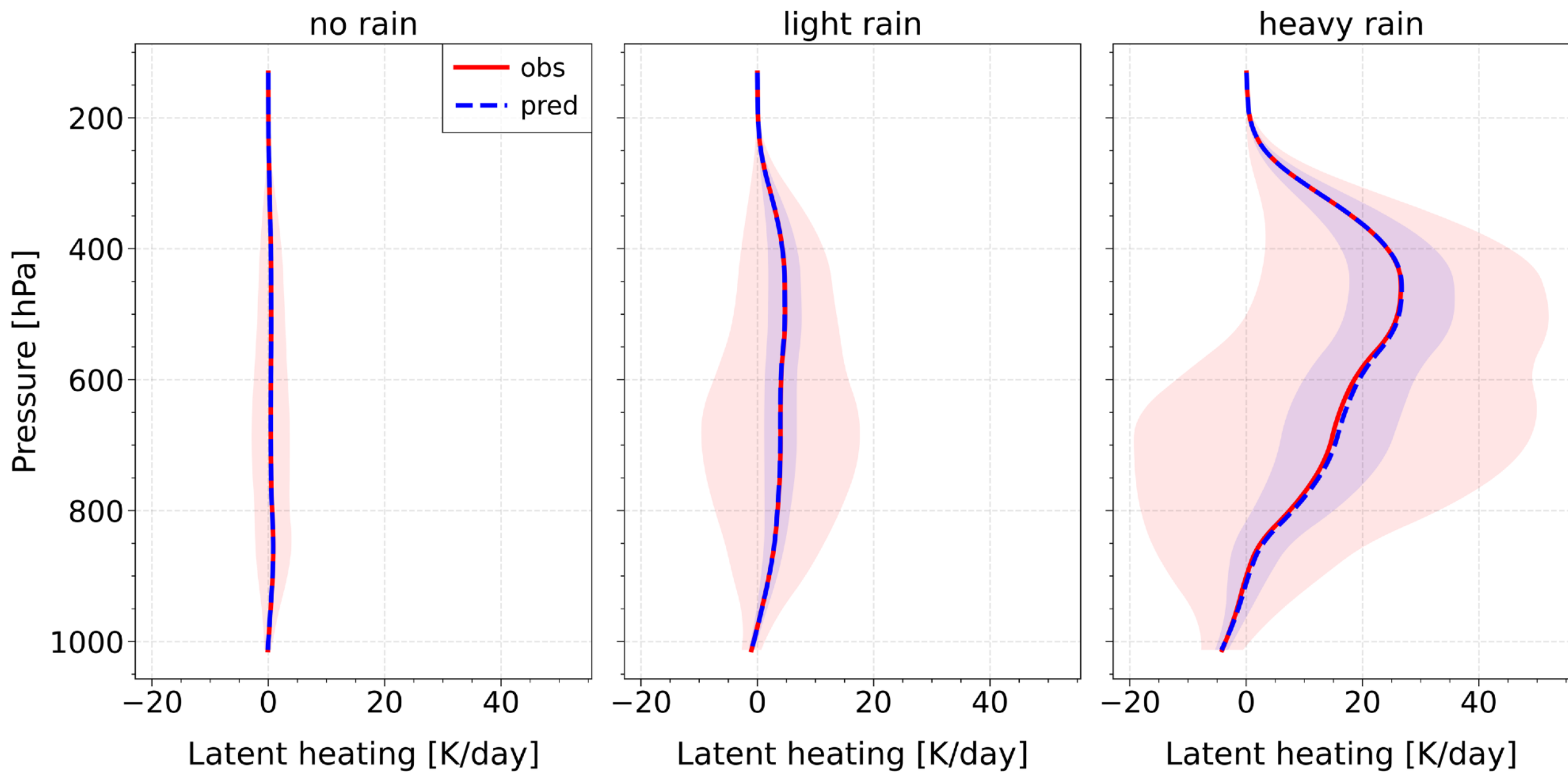
## LW Ocean



Good predicted mean,  
Underestimated predicted variability



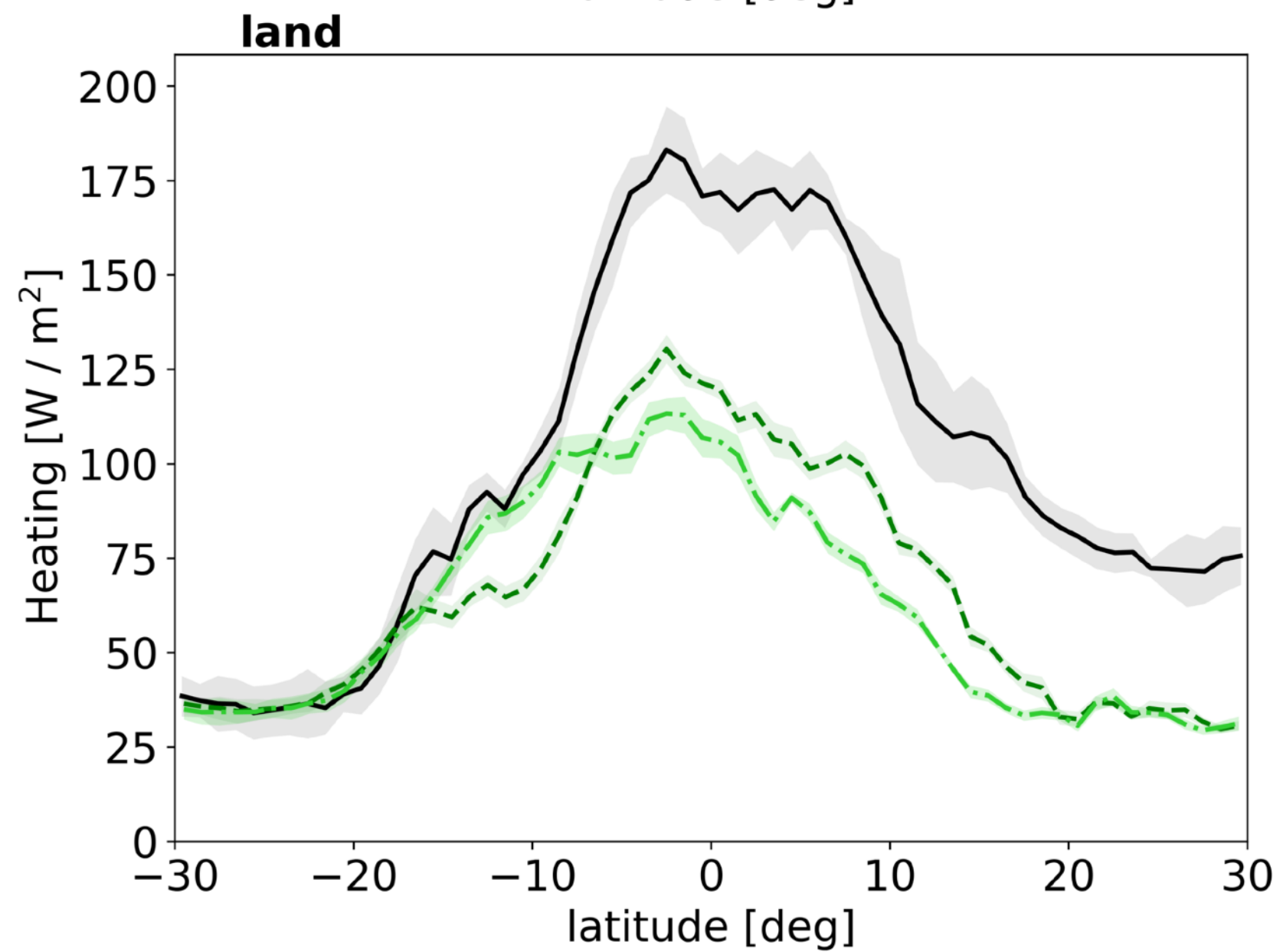
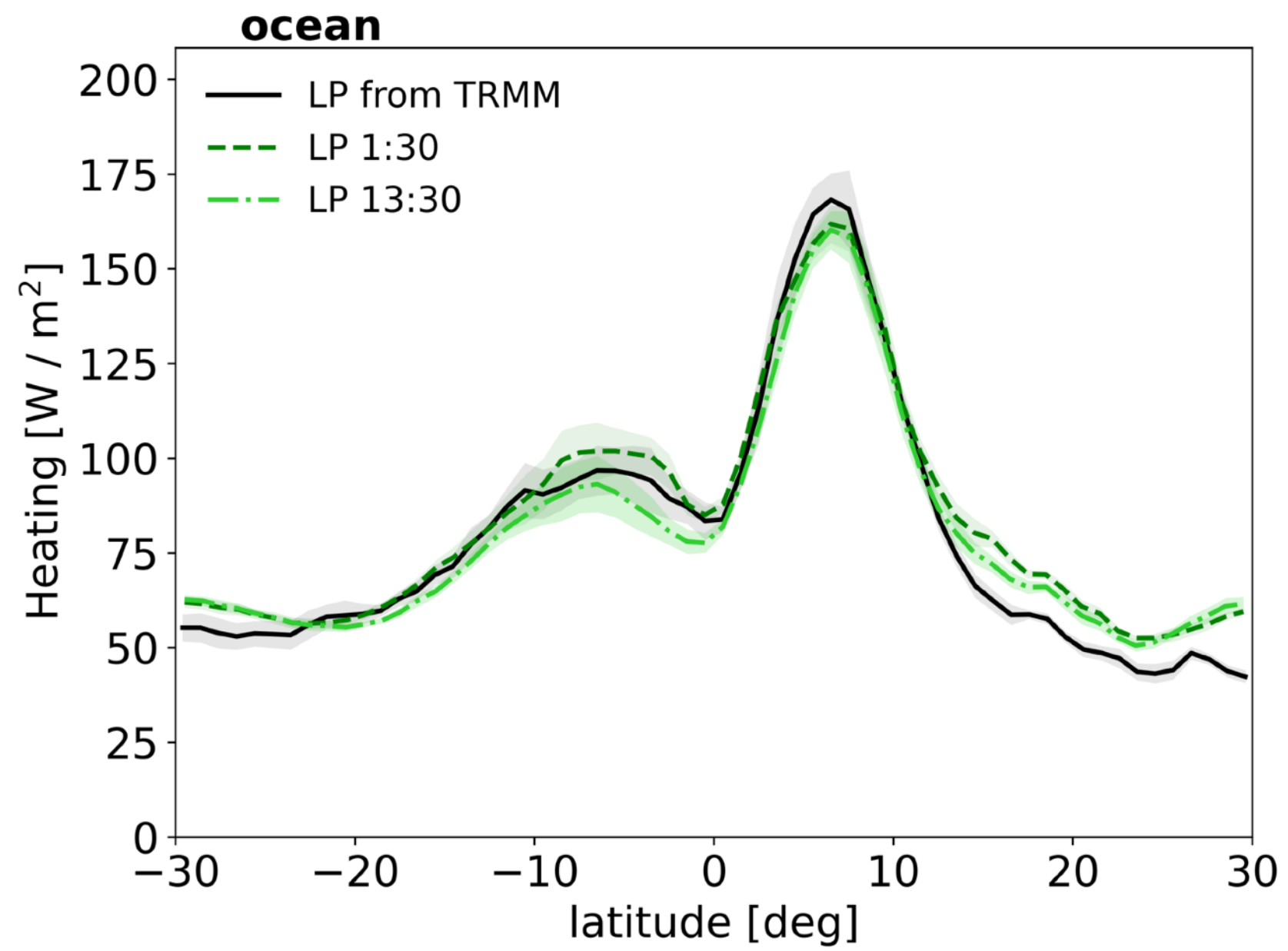
## LH Ocean



— LW radiative heating rates from Calipso-CloudSat  
- - - LW radiative heating rates from ANN prediction

— Latent heating rates from TRMM  
- - - Latent heating rates from ANN prediction

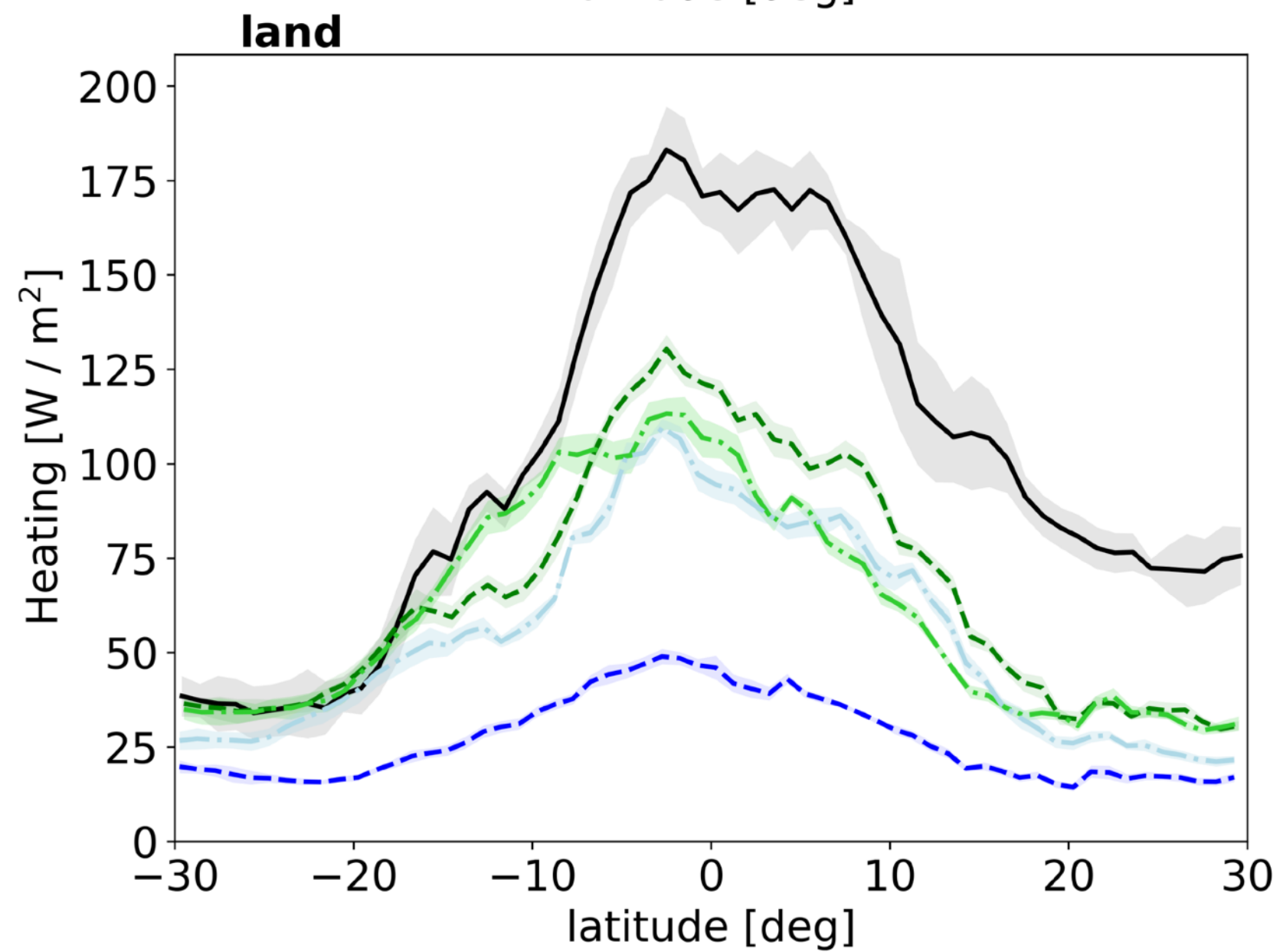
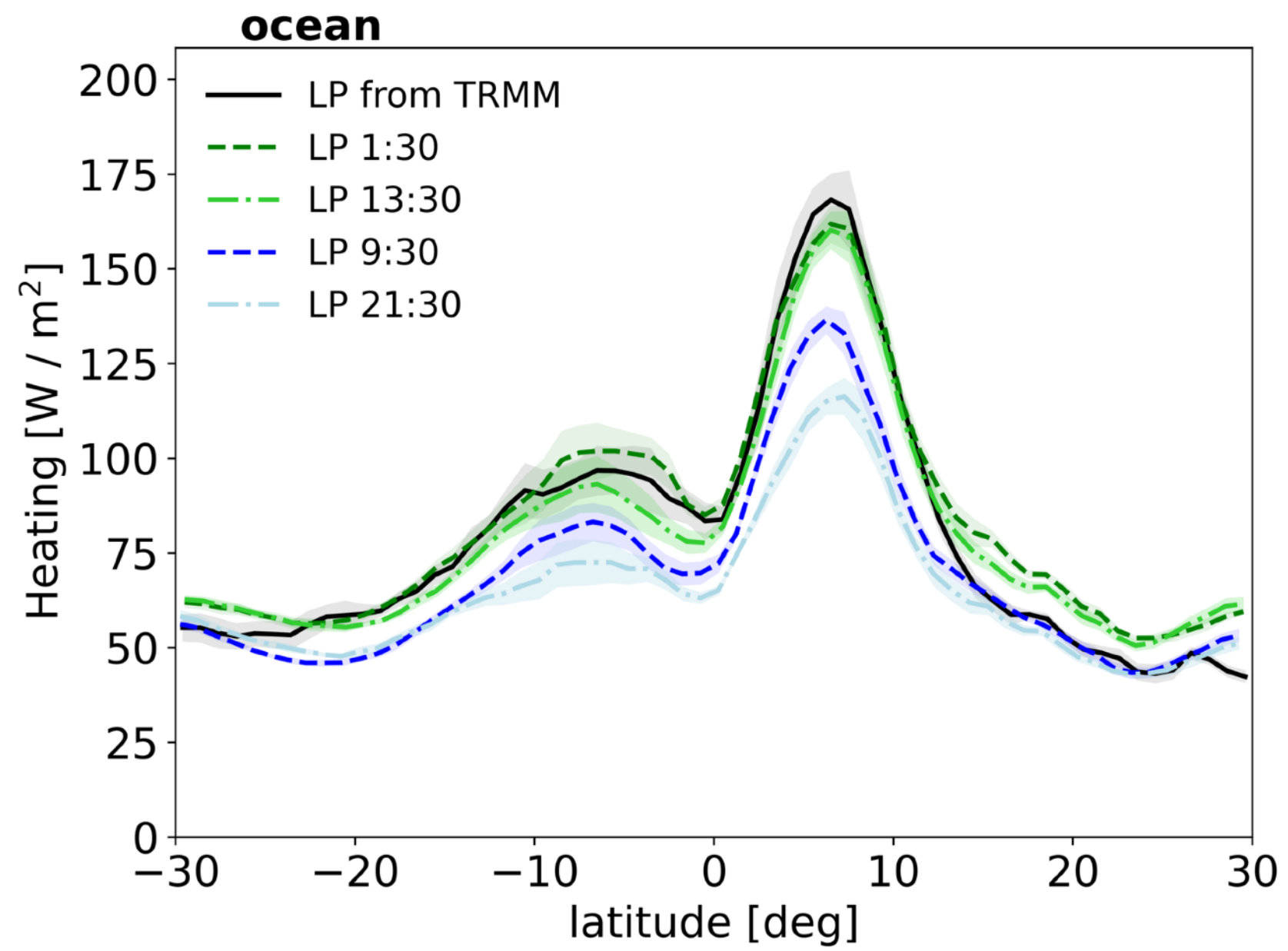
## Vertically integrated LH over all scenes



**Over ocean**, the zonal averages of LH at 1:30 AM&PM agree well with TRMM-SLH complete diurnal sampling.

**Over land**, we miss strong convection of late afternoon.

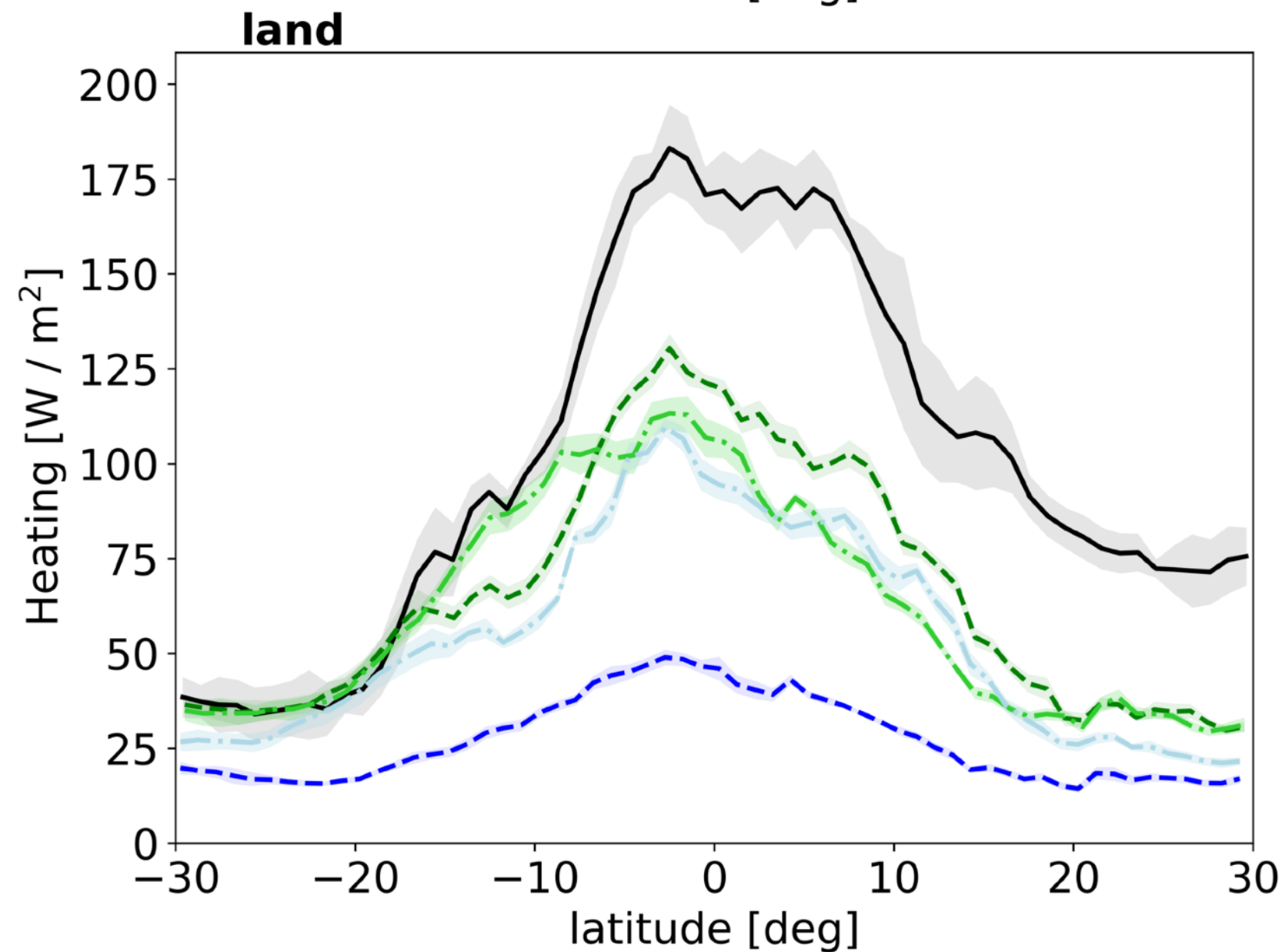
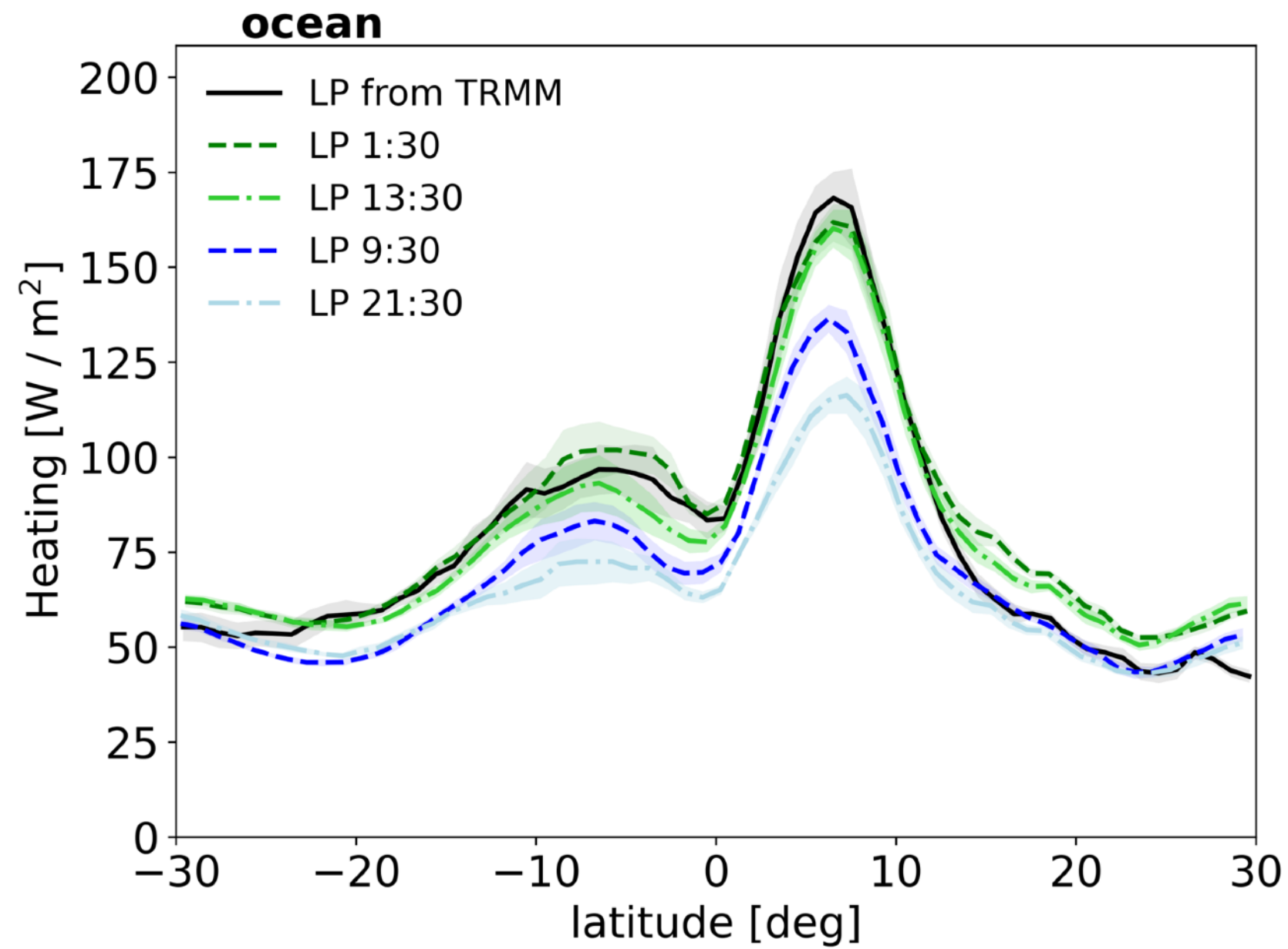
## Vertically integrated LH over all scenes



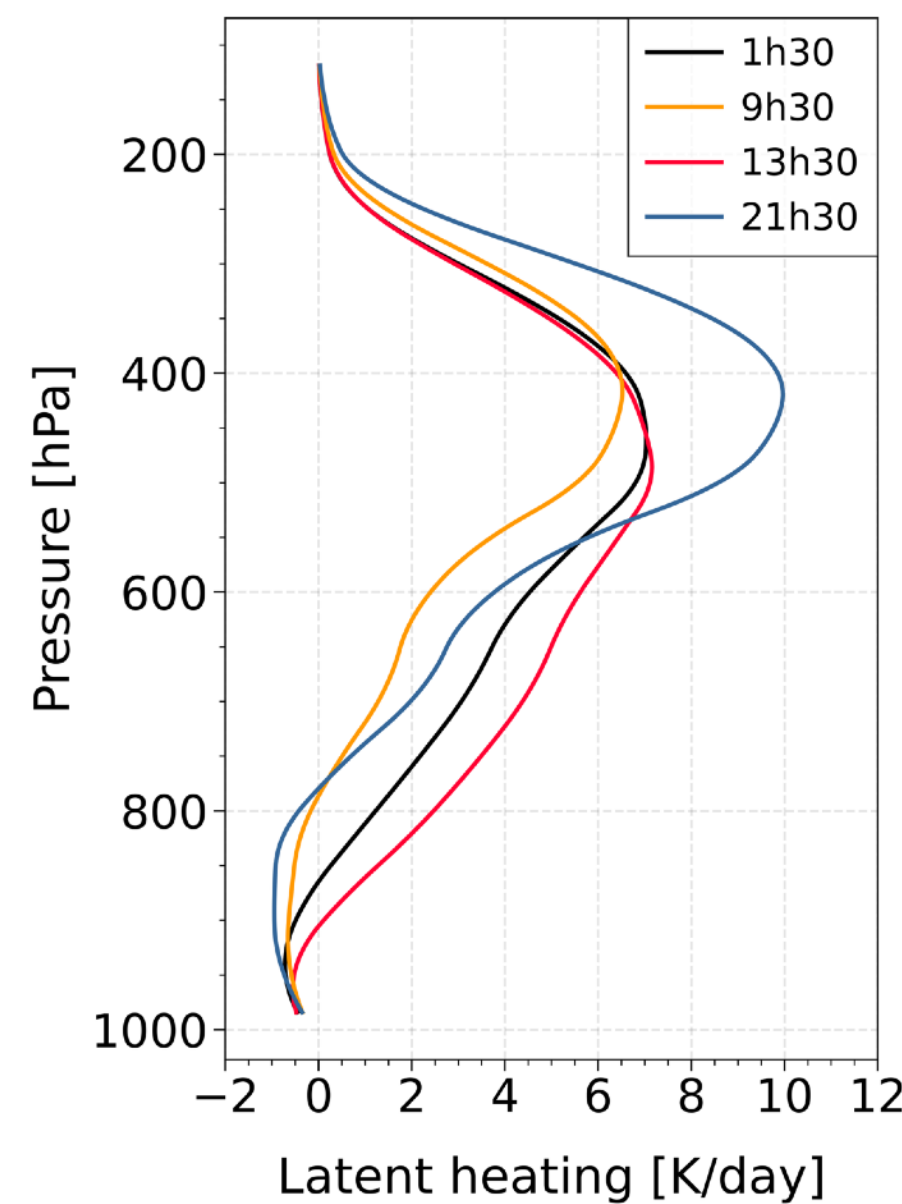
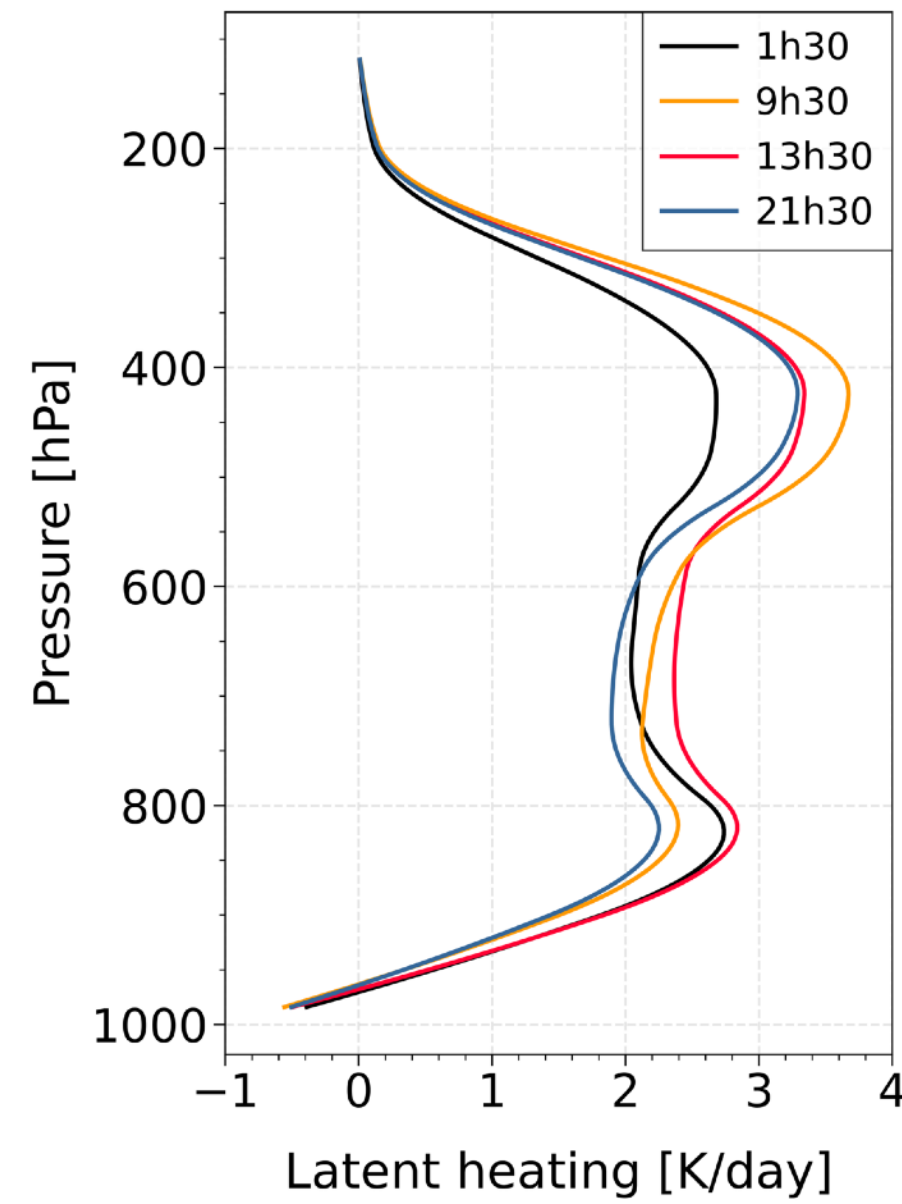
**Over ocean**, the zonal averages of LH at 1:30 AM&PM agree well with TRMM-SLH complete diurnal sampling.

While the sampling at 9:30 slightly underestimates LH

## Vertically integrated LH over all scenes



## LH profiles of rainy scenes



**Over ocean**, the zonal averages of LH at 1:30 AM&PM agree well with TRMM-SLH complete diurnal sampling.

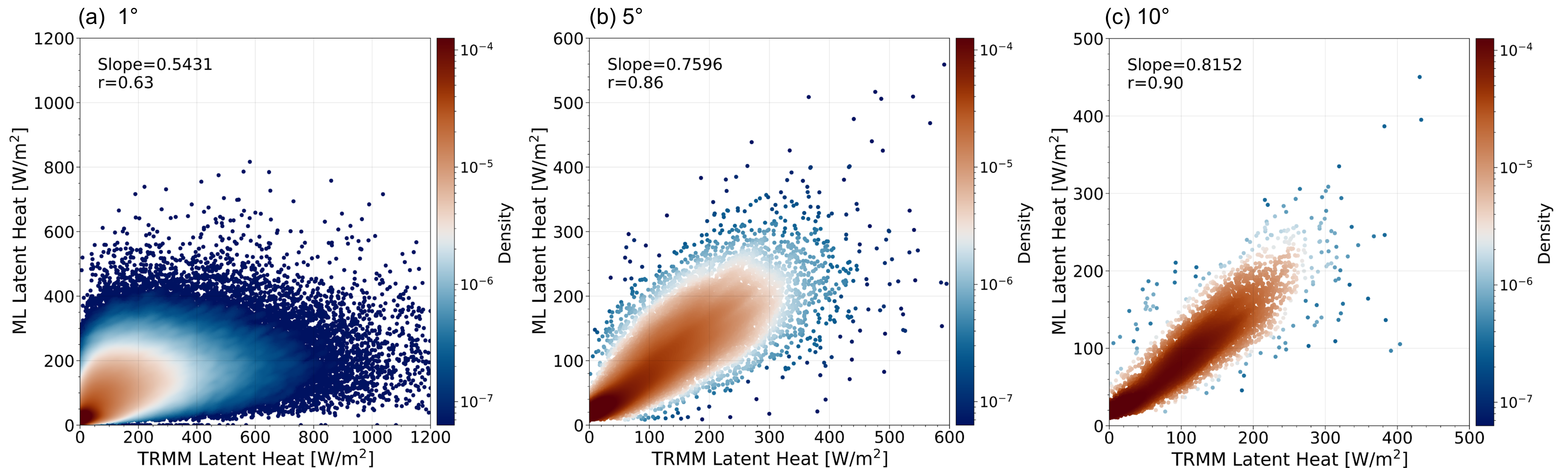
While the sampling at 9:30 slightly underestimates LH

**Shapes of ocean/land profiles** are different, as expected with a larger contribution of low level clouds over ocean.

### Diurnal cycle as expected:

Over ocean: maximum convection over early morning

Over land: maximum convection in the evening



- ❖ **The TRMM's revisit cycle strongly varies across regions**, with 23 days at the equator and up to 46 days at the highest latitudes (Negri et al., 2002).
- ❖ From **1° to 10°** averaging, slopes between TRMM-LP and ML-LP increase: **0.54 to 0.82 (10°N-10°S)**,  
**0.44 to 0.77 (20°N/S-30°N/S, not shown)**
- ❖ Strong bias reduction and noise reduction when averaging over more observations. For larger grid cell sizes the agreement is much better

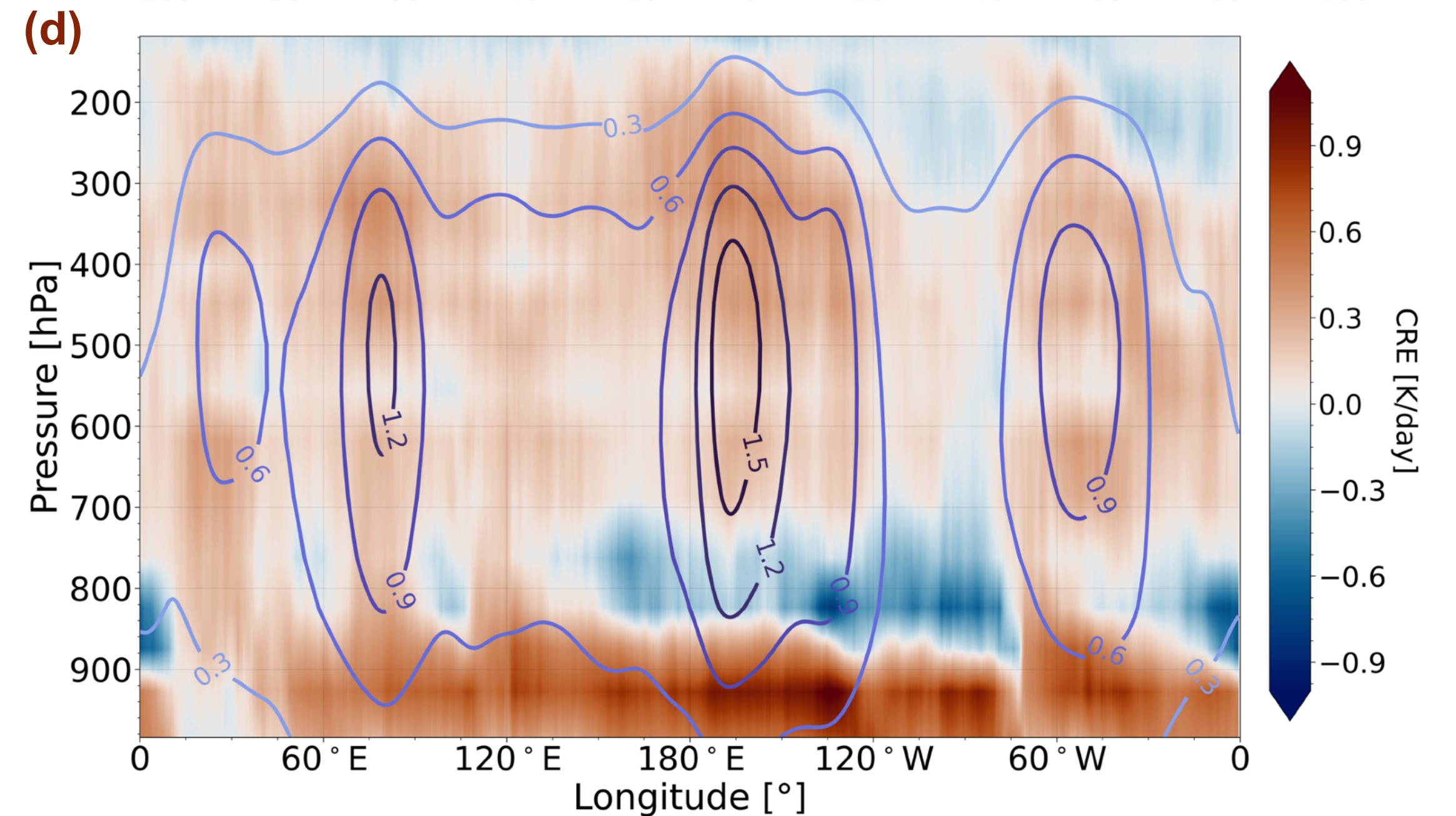
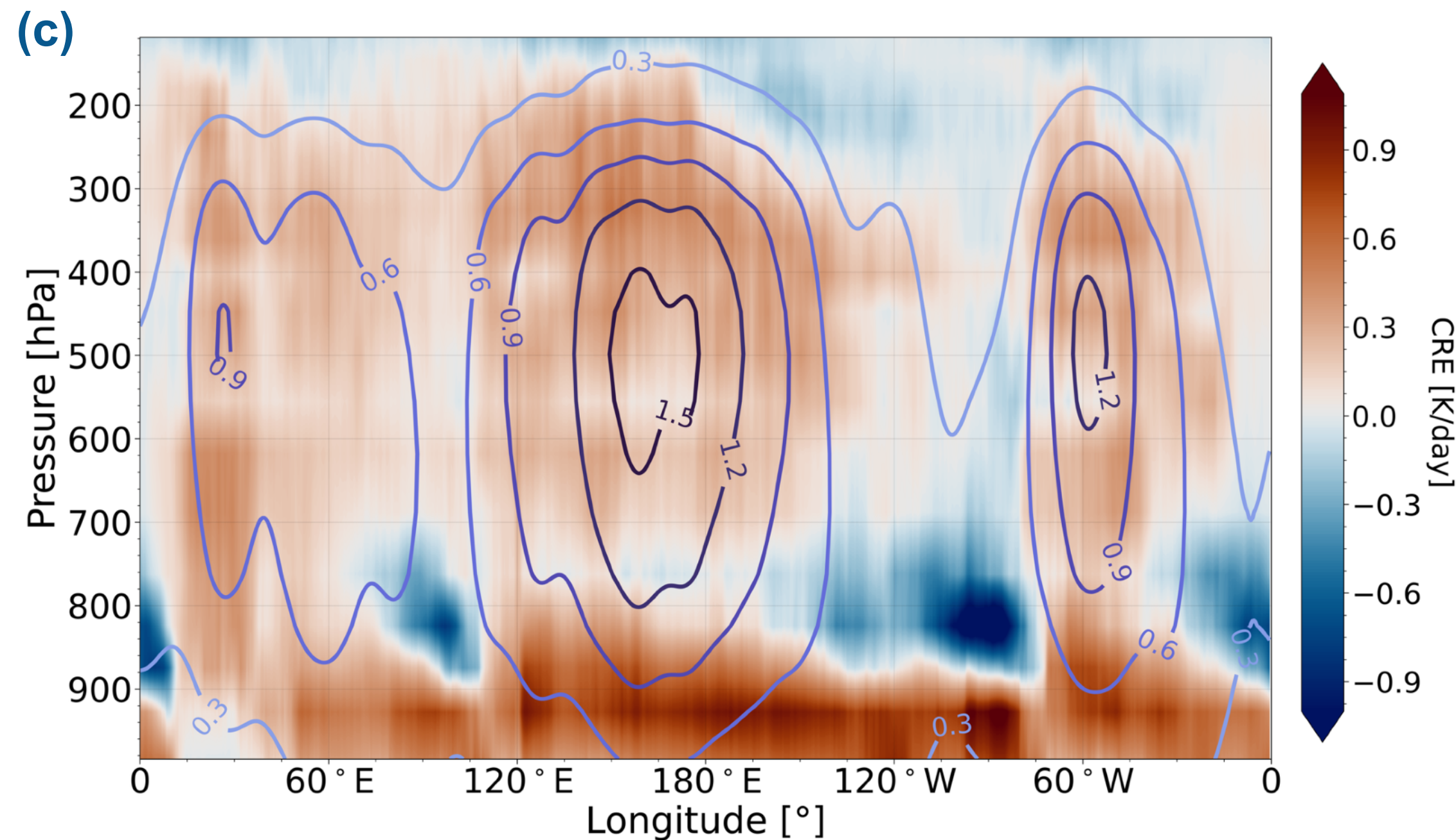
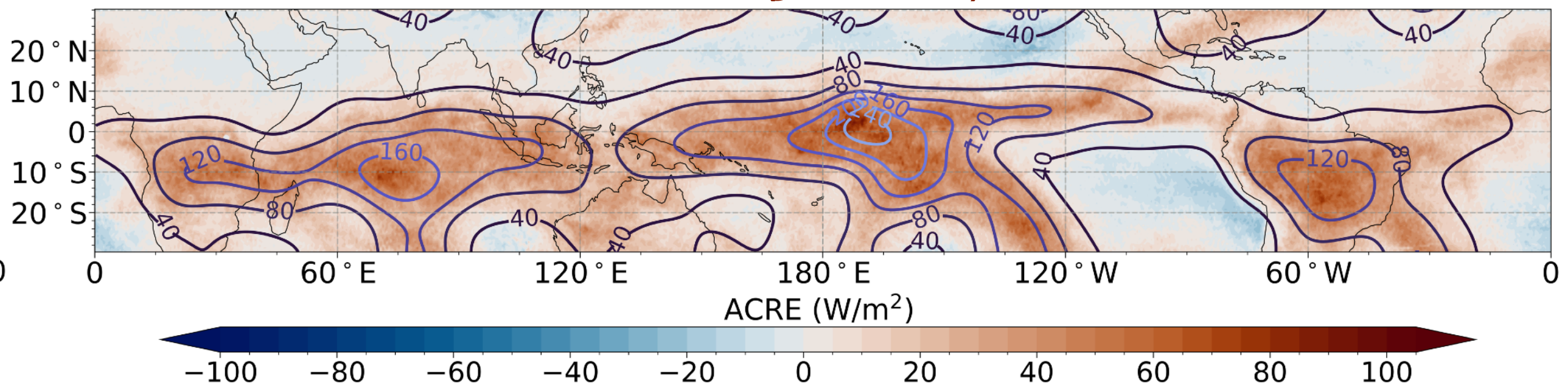
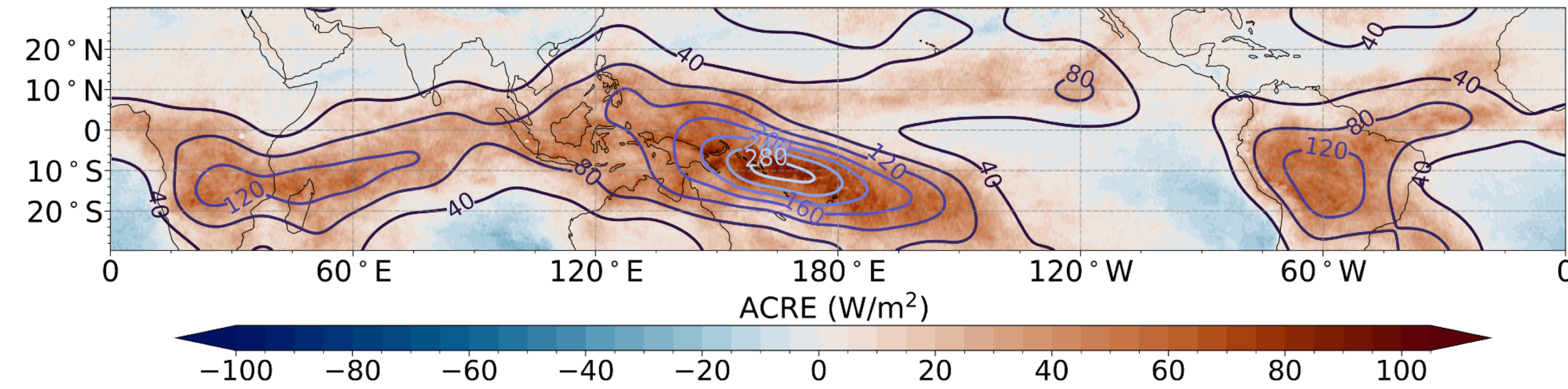
## Contrasting La Niña and El Niño events

**Atmospheric Cloud Radiative Effect (ACRE):** the difference in cloud radiative effects between the TOA and the surface

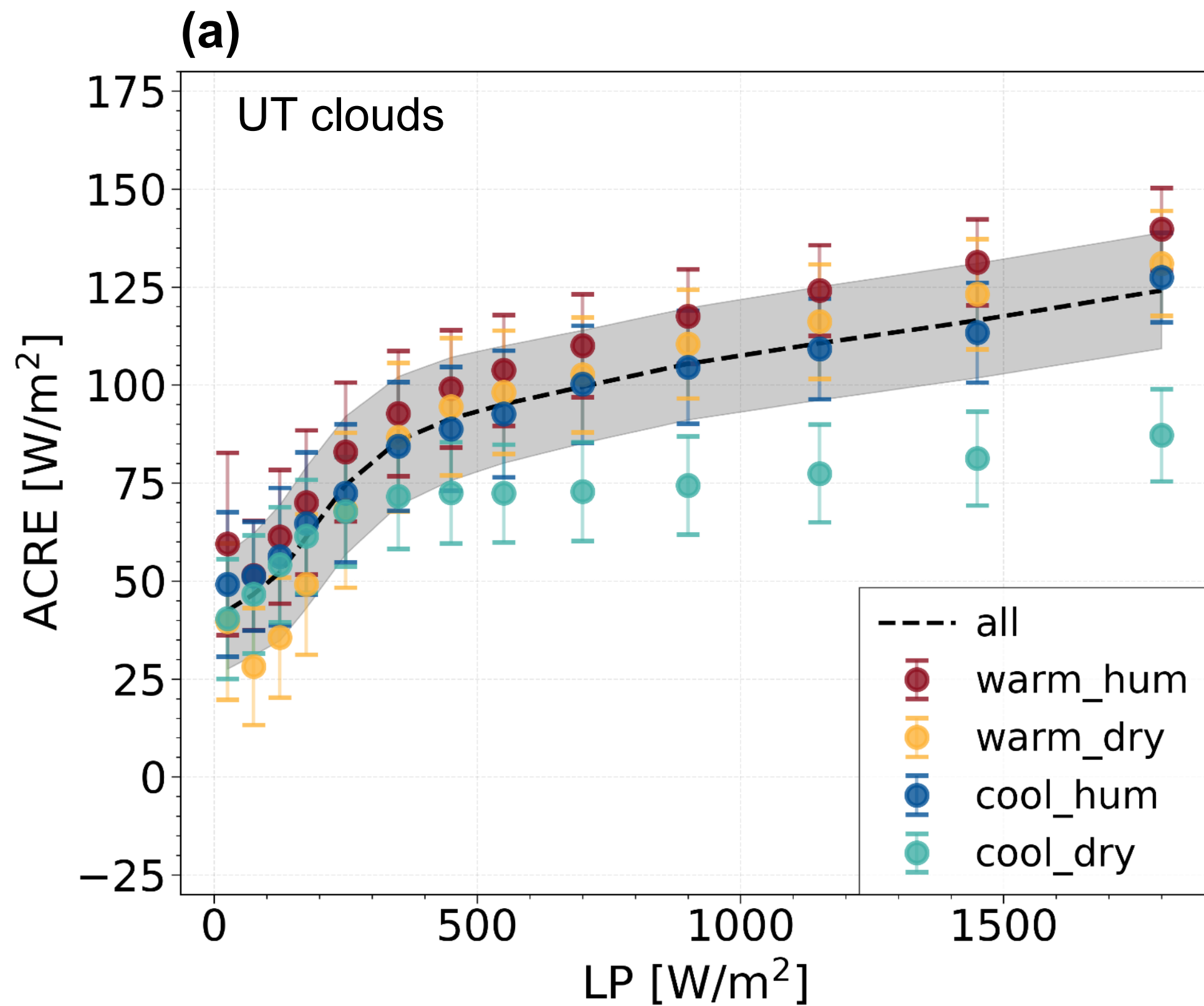
$$\text{ACRE} = \int \text{HR} \, dp - \int \text{HR}_{\text{clr}} \, dp$$

**(a) La Niña (Jan 2008)**

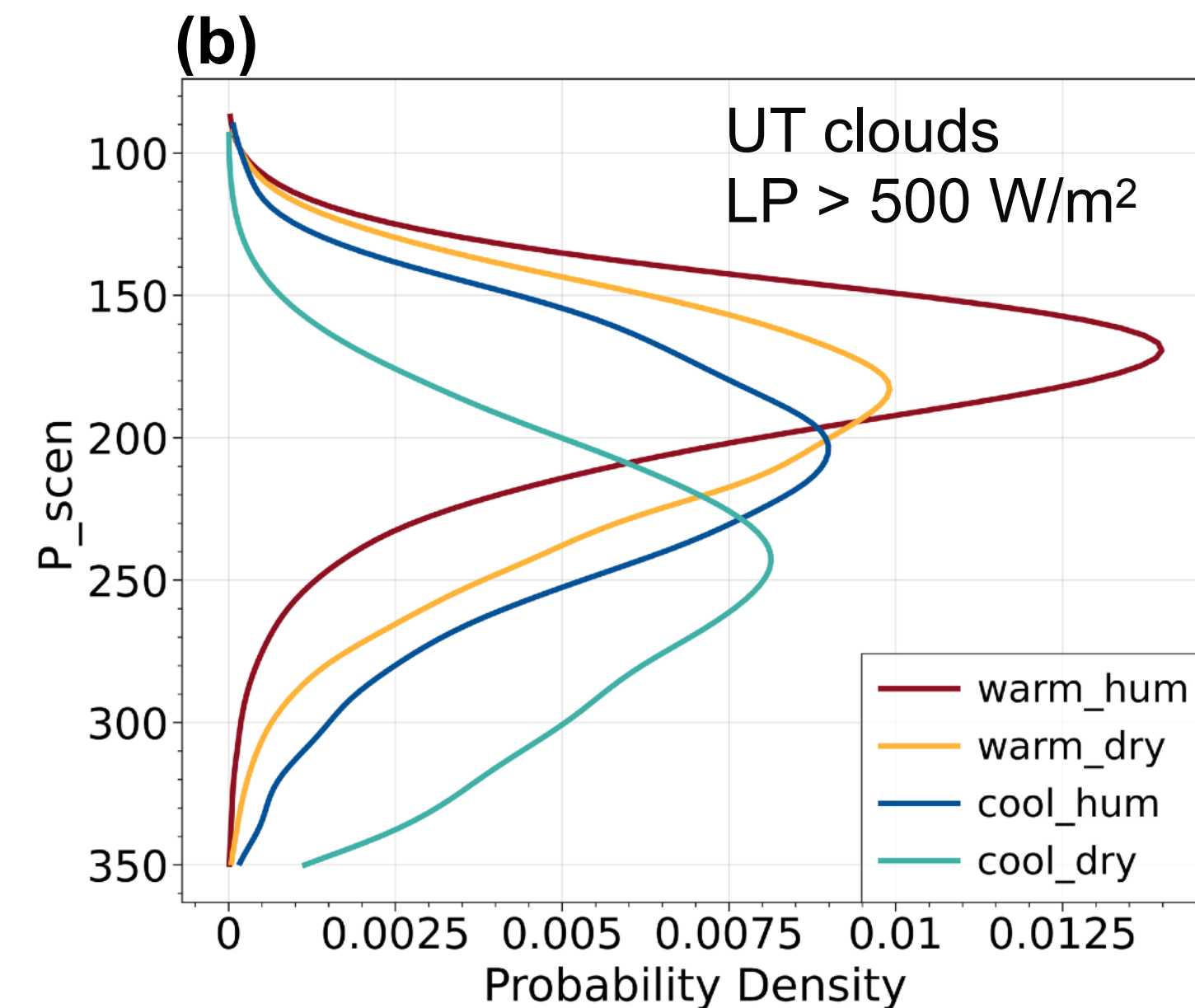
**(b) El Niño (Jan 2016)**



**Different environments characterized by sea surface temperature (SST) and **column water vapour (CWV)**:**

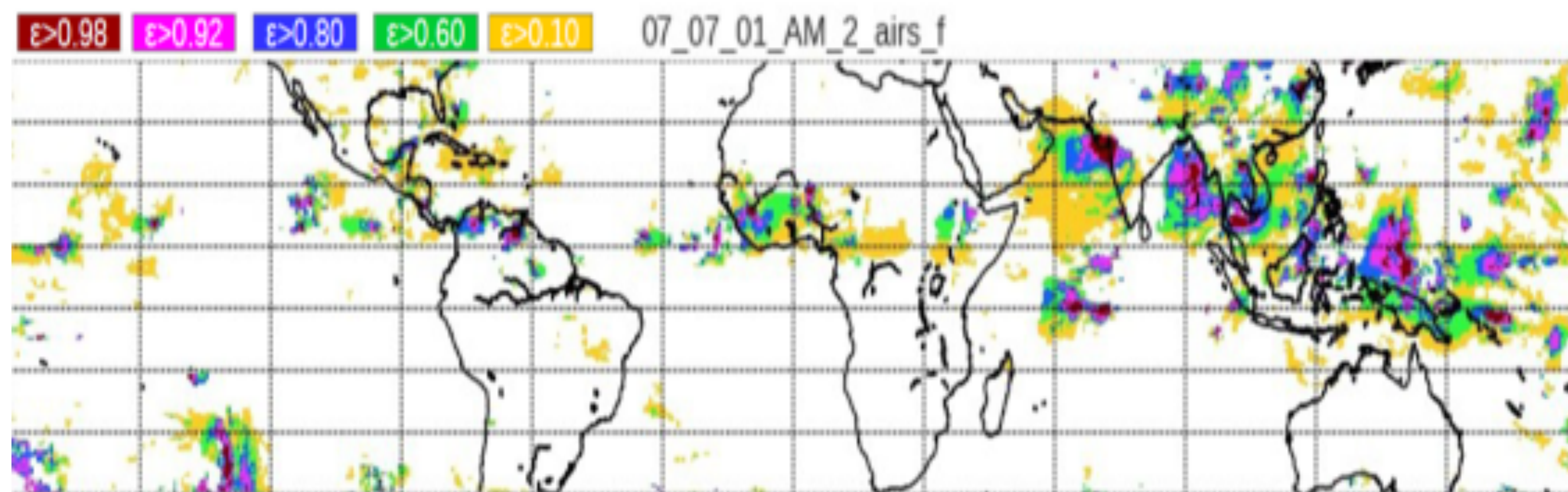
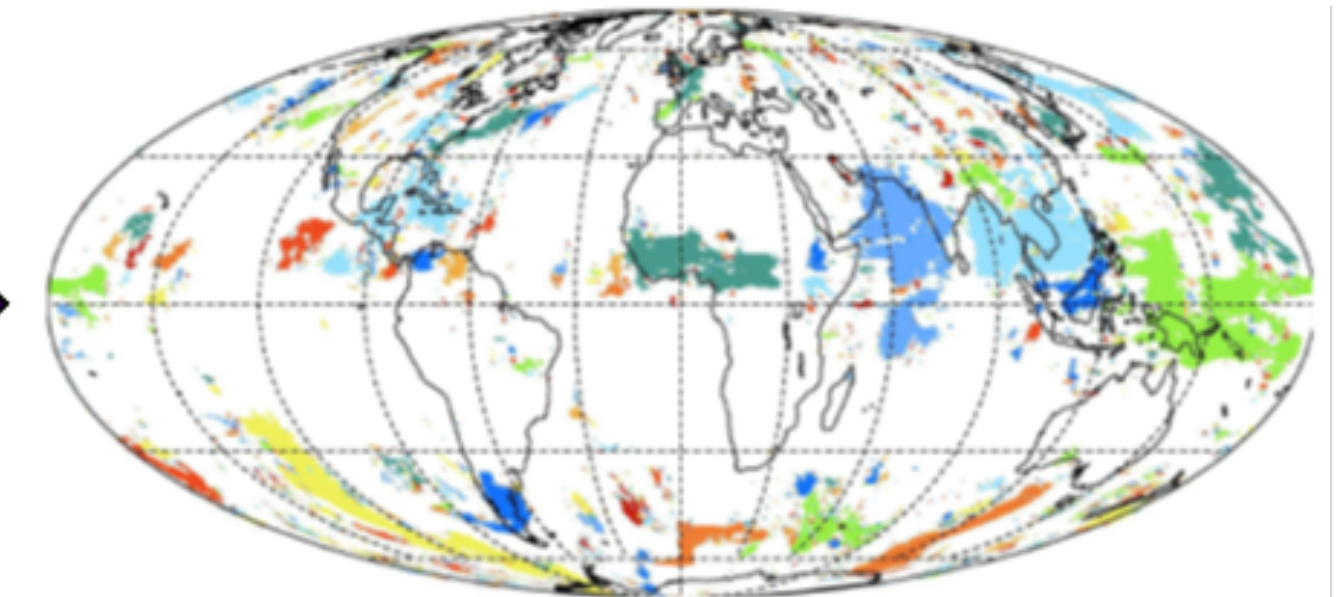
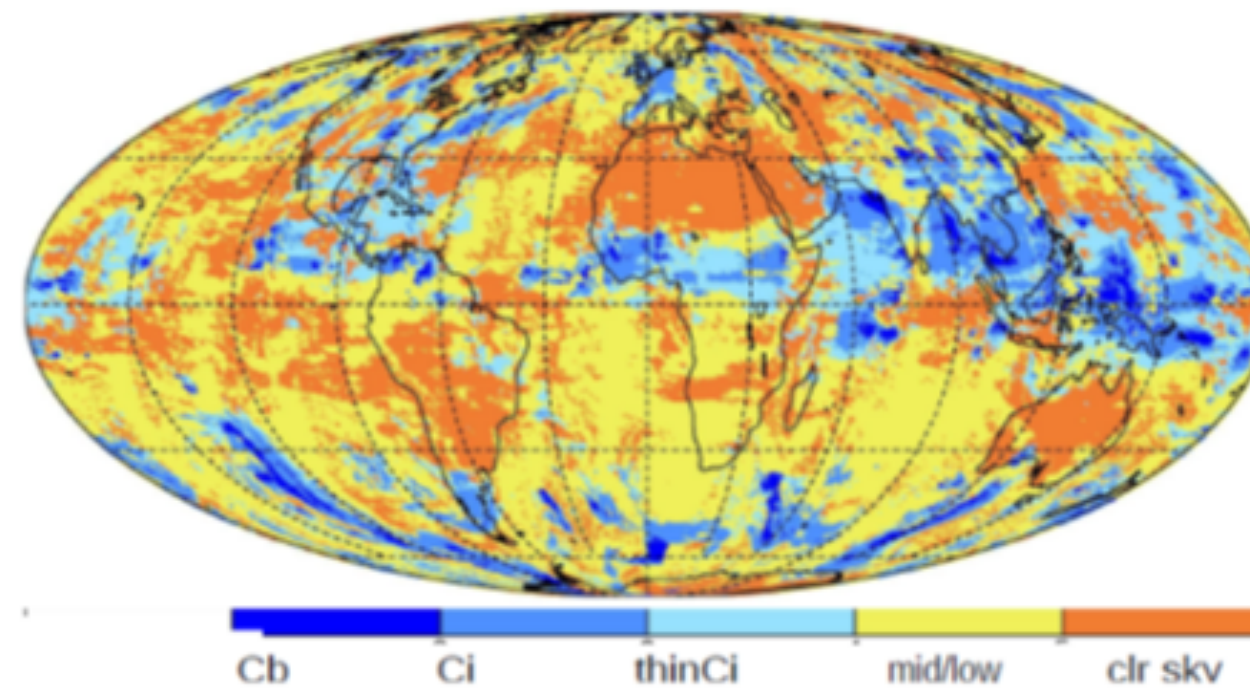
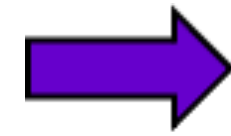
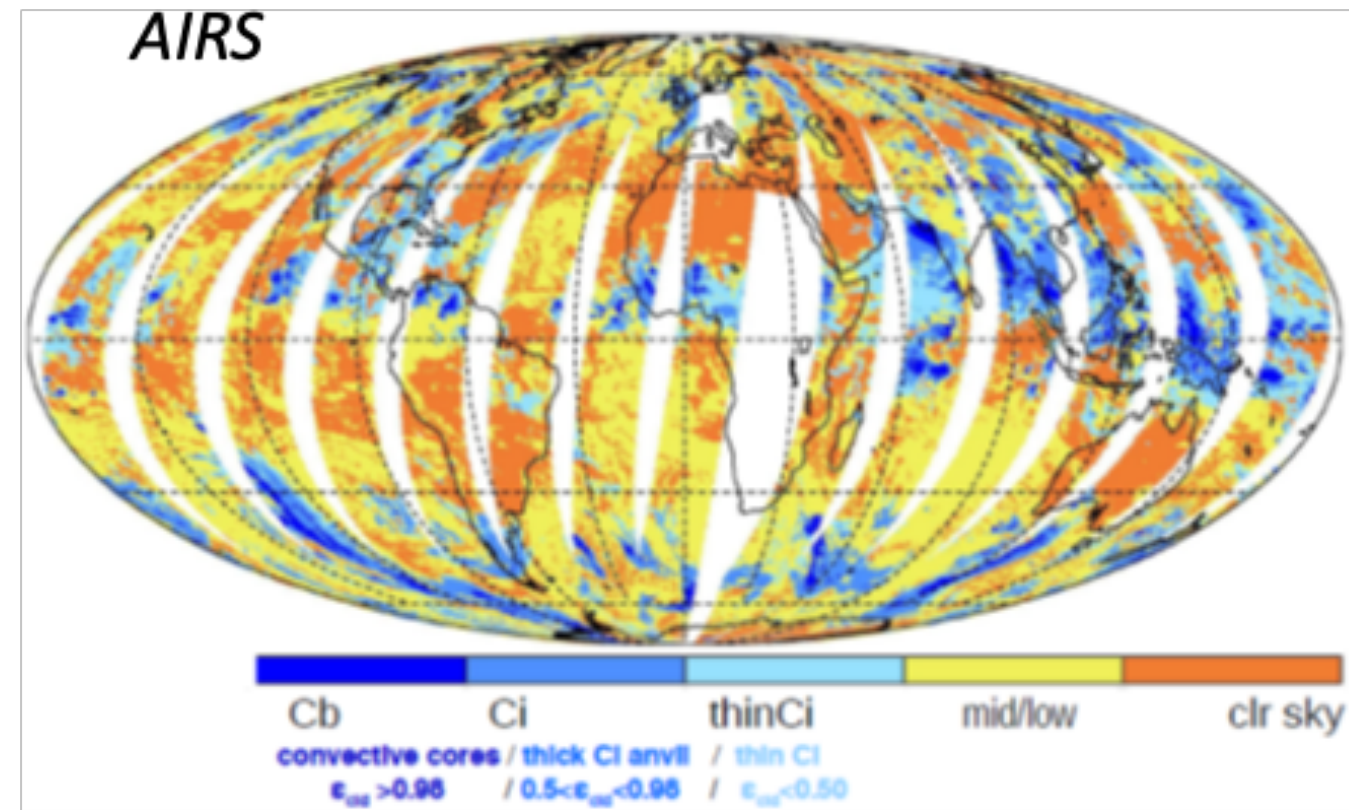


- ❖ For a given LP, **ACRE** is generally **largest** in **warm-humid** and **smallest** in **cool-dry** conditions.
- ❖ **SST** plays a **larger role** in **dry** environments.
- ❖ **Humidity** plays a **larger role** in **cool** environments.
- ❖ **Larger ACRE** is linked to **higher cloud height** (lower cloud top pressure).



**UT cloud systems** built from adjacent grid cells with similar  $P_{cld}$

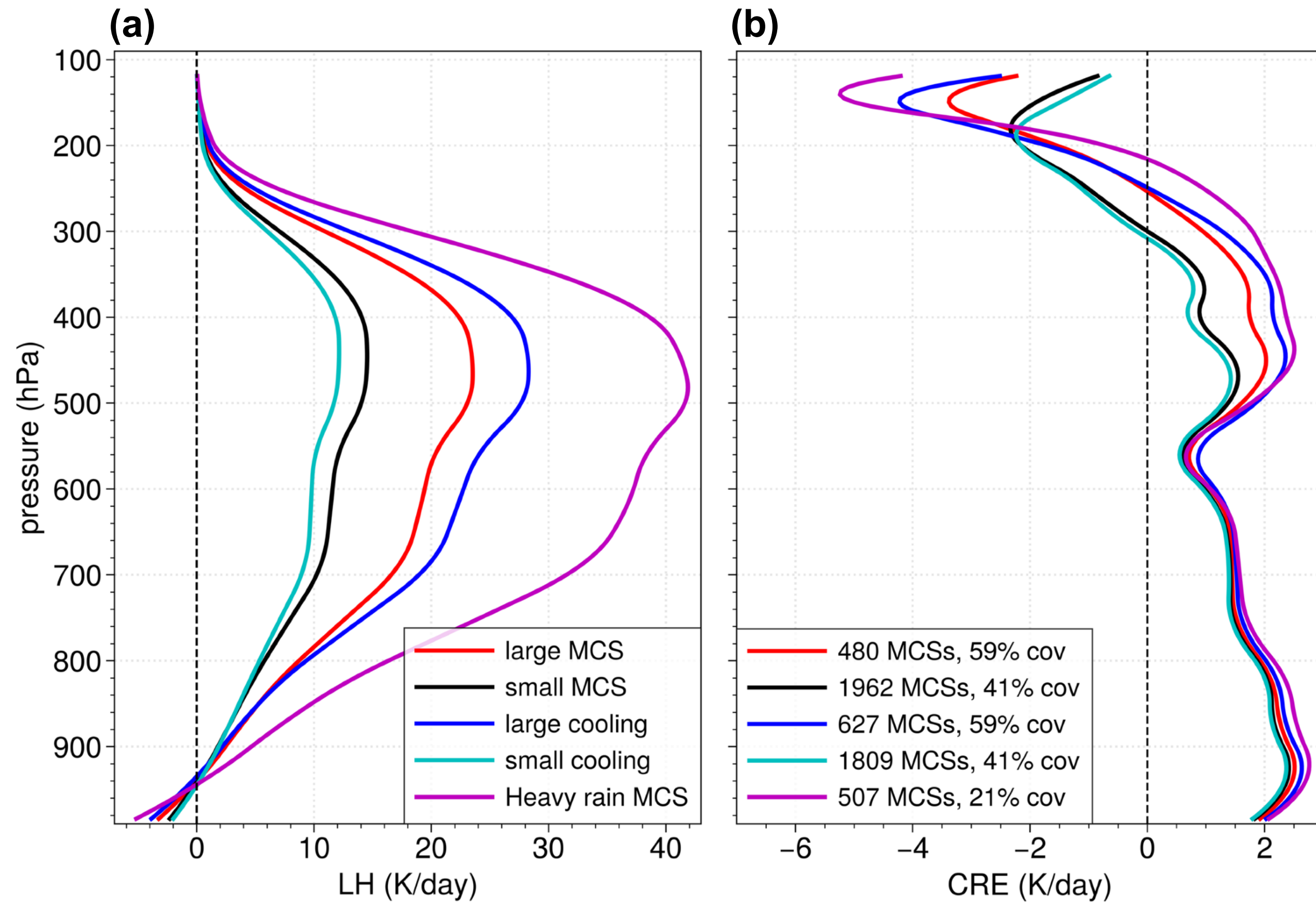
1 Jul 2007 AM



**Identification of MCS horizontal structure:**

Convective cores, Ci anvil & surrounding thin Ci from  $\epsilon_{cld}$

Grid cell resolution  $0.5^\circ$ ,  
sub-grid Cb, Ci, thin Ci fraction



**MCS reconstruction using CIRS  $P_{cld}$  and  $\epsilon_{cld}$**   
(Stubenrauch et al. 2023)

**Collocation with ML diabatic heating(only orbits)**



**Cooling above MCS core increases with opacity**  
**A proxy of deep convection**

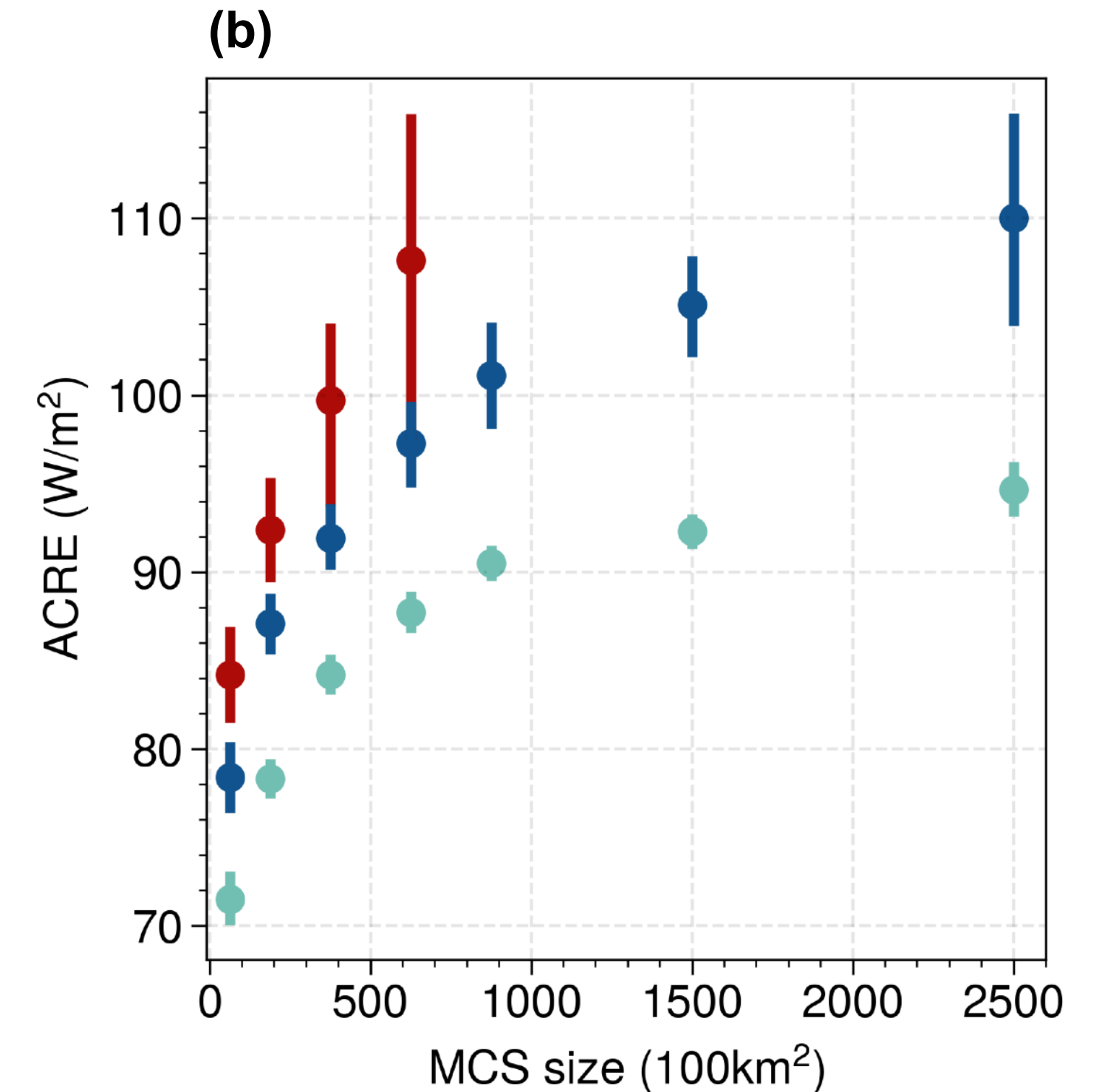
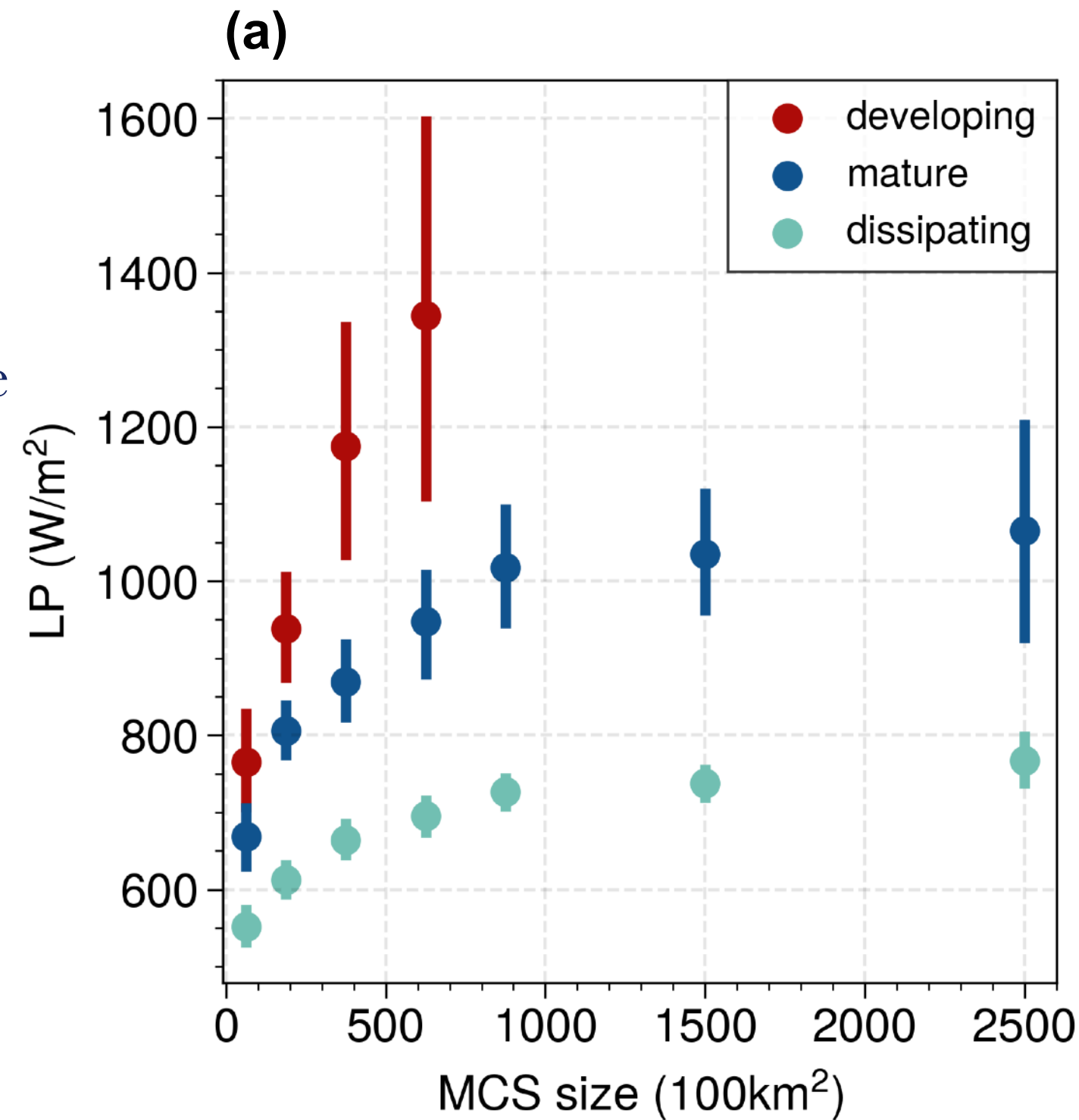
- ❖ Heavily raining MCS produce largest LH
- ❖ Deep convection can also be distinguished by large MCS size or large cooling above MCS cores

## Proxy for life stage:

### Convective core fraction within the MCS:

given by the ratio of convective core size over MCS size

- Developping** CF 0.6-0.9
- Mature:** CF 0.4-0.6
- Dissipating:** CF 0.2-0.4

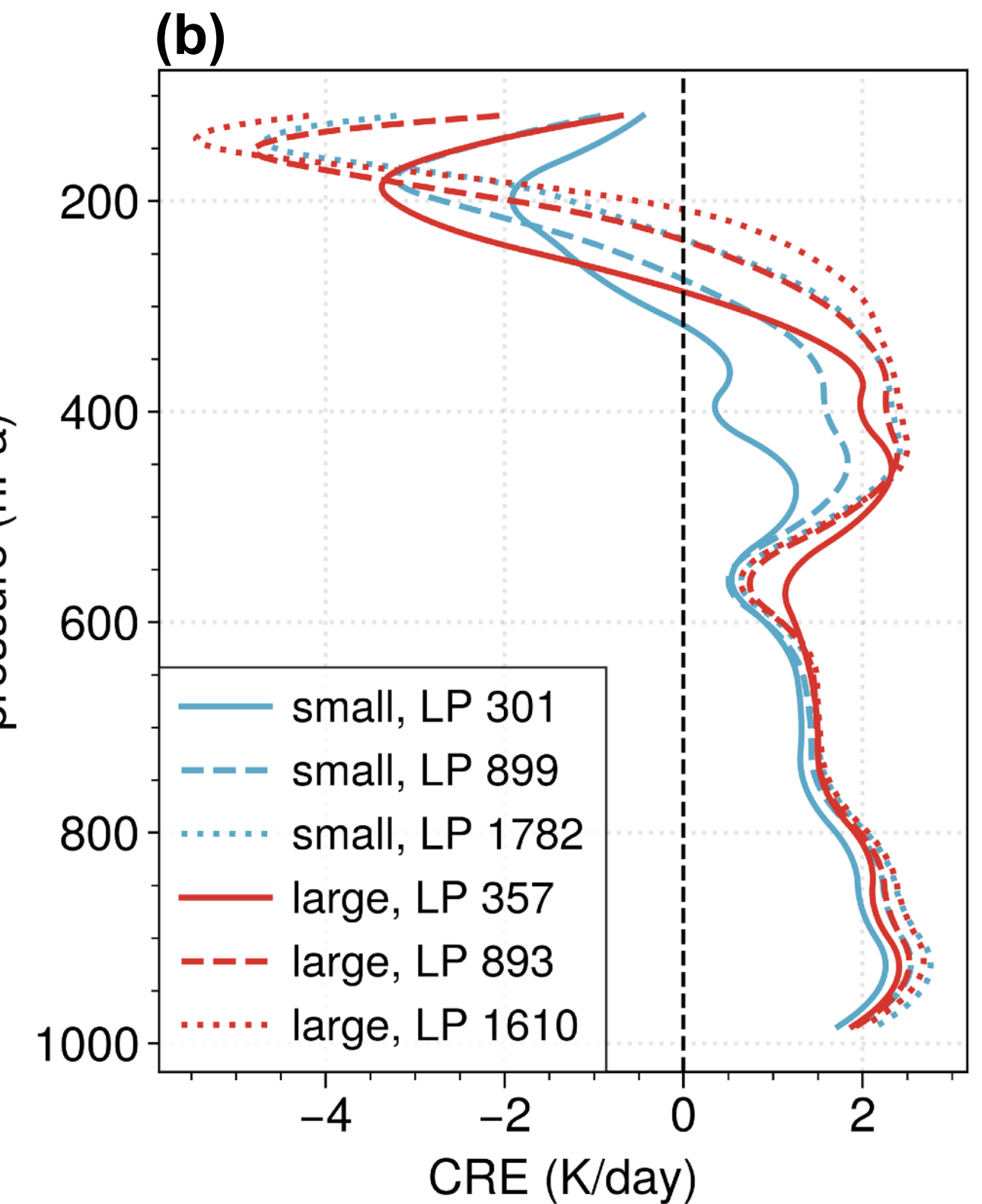
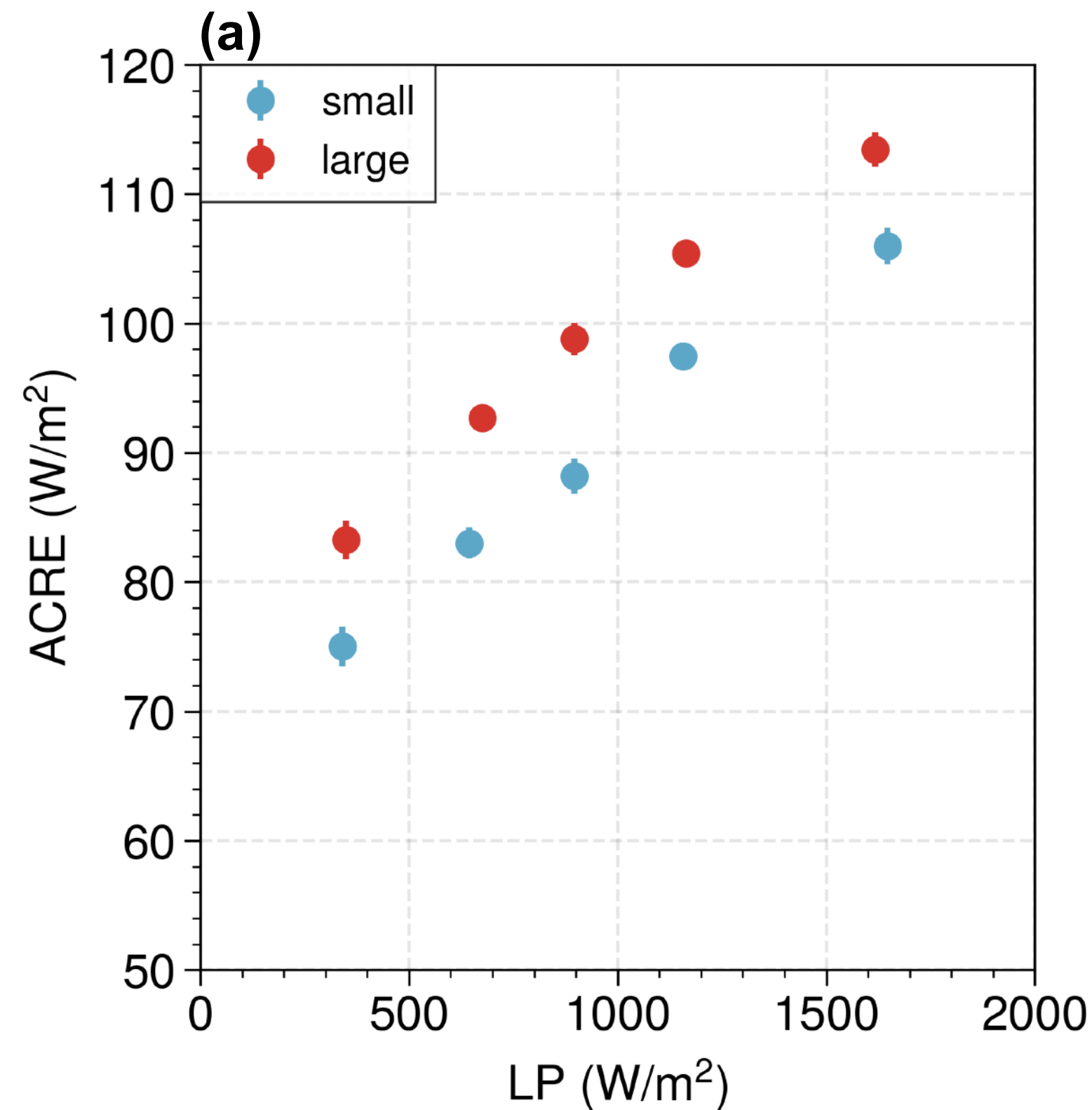


- ❖ Both LP and ACRE increase with MCS size, the increase flattens for larger MCS size.
- ❖ For a similar MCS size, LP and ACRE decrease from developing towards dissipating stage
- ❖ These behaviors are in line with those of the fraction of precipitation area within the MCS and the minimum temperature within the convective core, respectively.

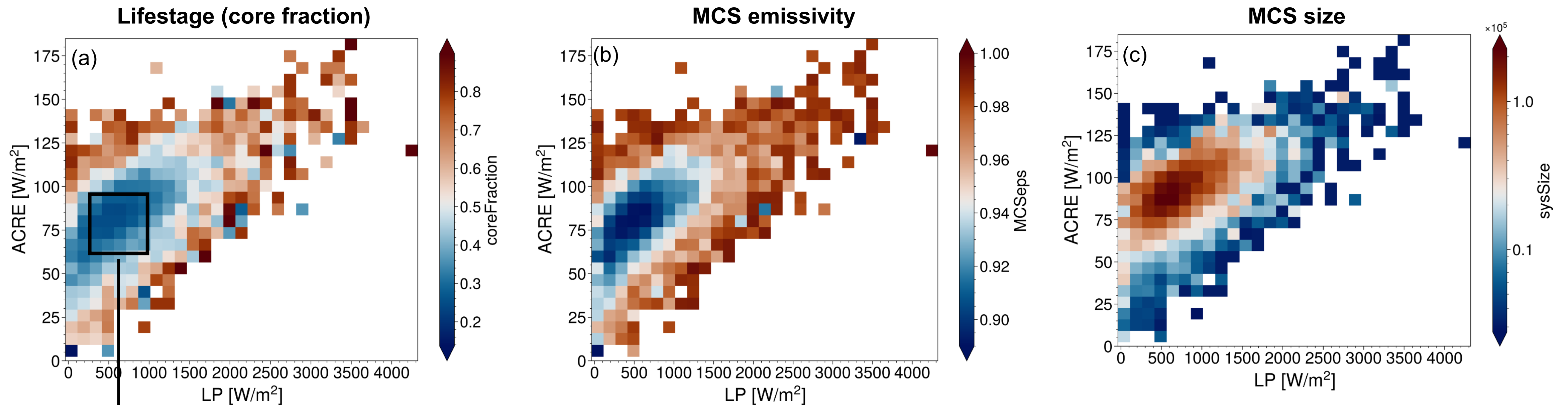
MCSs larger than 4 grid cells ( $1^\circ \times 1^\circ$ )

**Proxy for convective organisation:**  
MCS size at the same rain intensity (LP)

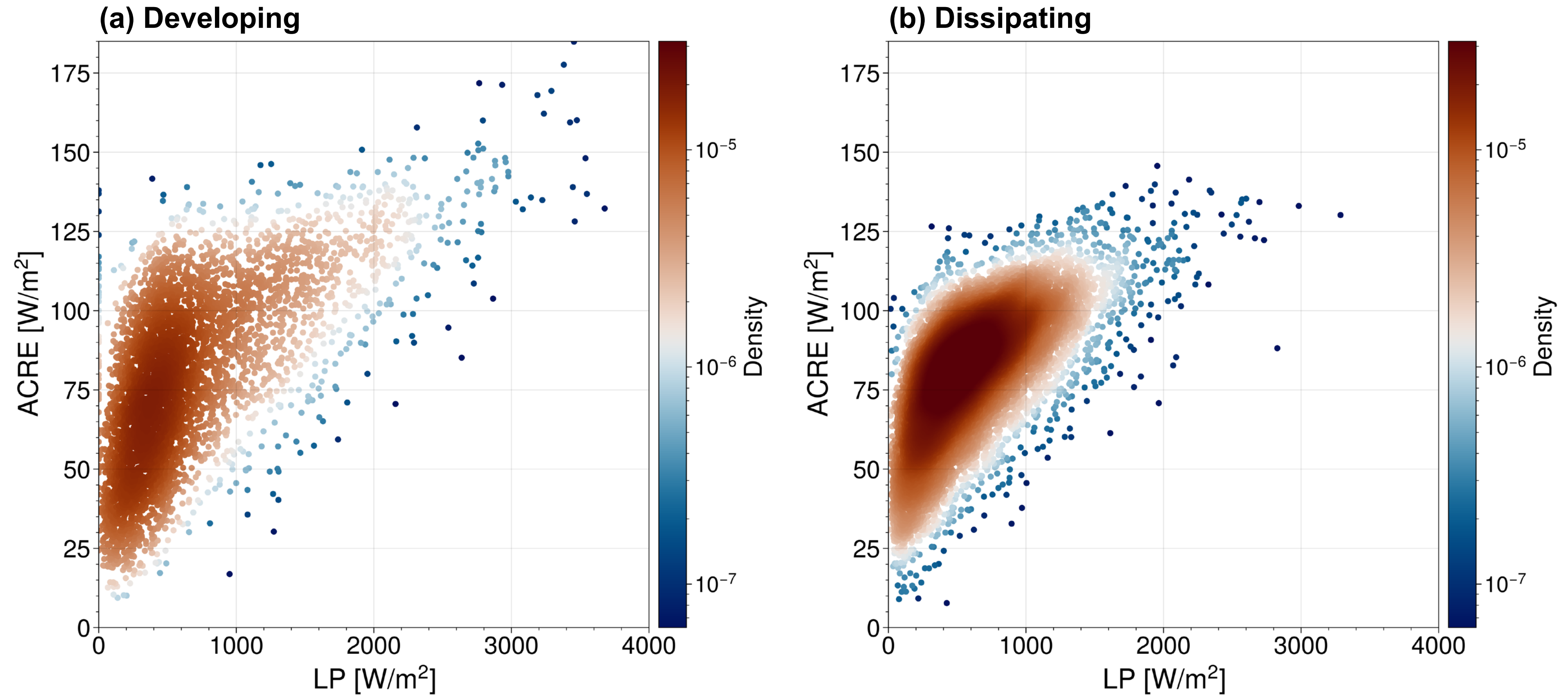
**Proxy for mature MCS:**  
Core Fraction: 0.4-0.6



- ❖ Convective organisation enhances ACRE by about  $10 Wm^{-2}$  for larger, more organised MCSs than for smaller, less organized MCSs at similar average rain intensity.
- ❖ More organized MCSs show larger vertical heating gradients at similar rain intensity.
- ❖ This additional ACRE and vertical heating gradients support stronger, sustained convection and impact large-scale environments.



- ❖ Masunaga and Takahashi (2024, GRL, under review): the MCSs converge during their evolution to a **settling point** with LP of about **700  $\text{Wm}^{-2}$**  and ACRE of about **75  $\text{Wm}^{-2}$** .
- ❖ Our MCS and life stage identifications are different, but a similar converging area can still be clearly observed:
  - ▶ MCSs with a larger core fraction and emissivity, smaller size occupy the LP-ACRE space at the border.
  - ▶ MCS in the later life stage (smaller core fraction and emissivity, larger size) occupy the LP-ACRE space closer to the settling point.



A broad scattering is in the LP-ACRE space of MCSs in the developing stage and a narrower distribution of MCSs is in the dissipating stage.

- ❖ We reconstructed longterm datasets of 3D radiative and latent heating at 4 observation times using ANN (2004-2018).
- ❖ While the mean and variability of radiative heating rates are well predicted, the mean of predicted latent heating rates agree well with observations but show smaller variability.
- ❖ Nevertheless, this expansion allows us to study horizontal fields of diabatic heating, in particular within MCSs.
- ❖ Convective organisation enhances ACRE by about  $10 \text{ Wm}^{-2}$ ; more organized MCSs show larger vertical heating gradients, supporting stronger and sustained convection.
- ❖ MCSs converge toward a mean LP-ACRE over their life cycle.

## **Future Plans:**

- ❖ Future studies should incorporate the time dimension (convection tracking).
- ❖ The distribution of MCS properties in the LP-ACRE plane could be used to investigate GCRM and GCM simulations.

- ❖ Chen, X., Stubenrauch, C. J., & Mandorli, G. (2024). Relationship between latent and radiative heating fields of tropical cloud systems using synergistic satellite observations. *EGUsphere*, 2024, 1–35. 10.5194/egusphere-2024-3434.
- ❖ Chen, X., Stubenrauch, C. J., & Mandorli, G. (2024). Diabatic heating of mesoscale convective cloud systems from synergistic satellite data, 2024 (Submitted to *IOP Conference Series: Earth and Environmental Science (EES)*)
- ❖ Stubenrauch, C. J., Mandorli, G., & Lemaitre, E. (2023). Convective organization and 3D structure of tropical cloud systems deduced from synergistic A-Train observations and machine learning. *Atmospheric Chemistry and Physics*. 23. 5867-5884. 10.5194/acp-23-5867-2023.
- ❖ Stubenrauch, C. J., Caria, G., Protopapadaki S.E., and Hemmer F. (2021). 3d radiative heating of tropical upper tropospheric cloud systems derived from synergistic a-train observations and machine learning. *Atmospheric Chemistry and Physics*, 21(2), 1015-1034.

❖

**Radiative heating rates are now available:**

***<https://gewex-utcc-proes.aeris-data/fr>***